2

indepth

Neurosurgery

Access the contents and videos on the online portal:
http://collections.medengine.com/neurology/in-depth-neurosurgery/

Springer Healthcare Education

START WITH

LEVESAM

Levetiracetam 250/500/750/1000mg Tablets • Levetiracetam Syrup/Injection 100mg/ml

EMPOWER HER

References: 1. Brodie MJ, *et al. Epileptic Disord.* 2003;5(Suppl 1):S65-S72.

COMPOSITION: Each film-coated tablet contains levetiracetam 250 mg / 500 mg / 750 mg /1000 mg. INDICATION: Adjunctive therapy in the treatment of partial onset seizures in adults with epilepsy. DOSAGE AND ADMINISTRATION: (Patients > 16 yrs of age) : Treatment should be initiated with a daily dose of 1000 mg/day, given as twice-daily dosing (500 mg BID), with or without food. Additional dosing increments may be given (1000 mg/day additional every 2 weeks) to a maximum recommended daily dose of 3000 mg, depending upon the clinical response and tolerability. Elderly: Adjust dose in patients with compromised renal function. Renal impairment: Adjust dose according to creatinine clearance. Hepatic impairment: No dose adjustment with mild to moderate hepatic impairment. CONTRAINDICATION: Hypersensitivity to levetiracetam or any ingredient of the formulation. WARNINGS AND PRECAUTIONS: Keep out of reach of children. Central nervous system adverse events, viz. somnolence and fatigue, coordination difficulties, psychotic symptoms and behavioral abnormalities reported to occur most frequently within the first 4 weeks of treatment. Minor hematologic abnormalities also reported. May cause dizziness and somnolence and hence jobs which require extreme alertness should be avoided. Withdrawal of drug: Gradual withdrawal advised. Pregnancy: Should be used only if the potential benefit justifies the potential risk to the fetus. Nursing Mothers: Because of the potential for serious adverse reactions in nursing infants, physician's discretion advised. Drug Interactions: No clinically significant interactions reported. ADVERSE REACTIONS: The most frequently reported adverse reactions are asthenia, headache, infection, pain, anorexia, amnesia, anxiety, ataxia, depression, dizziness, emotional liability, hostility, nervousness, paresthesia, somnolence, vertigo, increased cough, pharyngitis, rhinitis, sinusitis, diplopia. HOW SUPPLIED / STORAGE: Blister pack of 10 tabs. Store in a cool, dry place, protected from light. Please read the full prescribing information before usage. Additional information available on request with the Medical Services Division, Abbott Healthcare Private Limited, 1st Floor, D Mart Building, Goregaon-Mulund Link Road, Mumbai 400080. Version: 1.06, Dt. 05-04-16

Abridged Prescribing Information: LEVESAM ORAL SOLUTION
COMPOSITION: Each 1 ml contains levetiracetam 100 mg. INDICATION: Adjunctive therapy in the treatment of partial onset seizures in adults in adults and children 4 years of age and older with epilepsy. DOSAGE AND ADMINISTRATION: (Patients > 4 years of age): Treatment should be initiated with a daily dose of 20 mg/day in 2 divided doses(10 mg/kg BID). The daily dose should be increased every 2 weeks by increments of 20 mg/kg to the recommended daily dose of 60 mg/kg, the daily dose may be reduced. Patients with body weight ≤20 kg should be dosed with oral solution. Levetiracetam is given orally with or without food. (Patients >16 yrs of age): Treatment should be initiated with a daily dose of 1000 mg/day, given as twice-daily dosing (500 mg BID), with or without food. Additional dosing increments may be given (1000 mg/day additional every 2 weeks) to a maximum recommended daily dose of 3000 mg. CONTRAINDICATION: Hypersensitivity to levetiracetam or any ingredient of the formulation. WARNINGS AND PRECAUTIONS: Keep out of reach of children. Central nervous system adverse events, viz. somnolence and fatigue, coordination difficulties, psychotic symptoms and behavioral abnormalities reported to occur most frequently within the first 4 weeks of treatment. Minor hematologic abnormalities also reported. May cause dizziness and somnolence and hence jobs which require extreme alertness should be avoided. Withdrawal of drug: Gradual withdrawal advised. Pregnancy: Should be used only if the potential benefit justifies the potential risk to the fetus. Nursing Mothers: Because of the potential for serious adverse reactions in nursing infants, physician's discretion advised. Drug Interactions: No clinically significant interactions reported. ADVERSE REACTIONS: The adverse events most frequently reported with the use of Levetiracetam in combination with other AEDs in pediatric patients were somnolence, accidental injury, hostility, nervousness and asthenia. The most frequently reported adverse events associated with the use of levetiracetam in combination with other AEDs in adults were somnolence, asthenia, infection and dizziness. Of the most frequently reported adverse events in adults were asthenia, somnolence and dizziness is reported to occur predominantly during the first 4 weeks of treatment with levetiracetam. HOW SUPPLIED / STORAGE: Syrup is available in bottle pack of 100 ml. Store in a cool, dry place, protected from light. Keep out of reach of children.

Please read the full prescribing information before usage.
For additional information, please contact Medical Services Division,
Abbott Healthcare Pvt. Ltd.
Floor 18, Godrej BKC, Plot No. C-68, Near MCA Club, Bandra-Kurla Complex, Bandra East, Mumbai 400051. www.abbott.co.in

Version : 1.0, Dt. 19.06.2014

Abbott

INDLVM185007a 28 NOV 2018

indepth

Neurosurgery

Springer Healthcare Education

April 2019

Springer Healthcare

This edition is created in India for free distribution in India.
This edition is published by Springer Nature India Private Limited.
Registered Office: 7th Floor, Vijaya Building, 17, Barakhamba Road, New Delhi 110 001, India.
T: +91 11 4575 5888
www.springerhealthcare.com

Part of the Springer Nature group

Contents

Step by step procedure to view the online contents and video/s:

1. Go to http://collections.medengine.com/neurology/in-depth-neurosurgery/ or scan QR code.

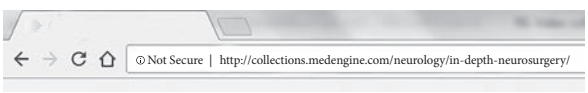

2. Web page of the issue will be opened.

3. You can read the PDF and view the video/s online. Both can be downloaded also.

Frameless Robot-assisted Stereoelectroencephalography for Refractory Epilepsy in Pediatric Patients: Accuracy, Usefulness, and Technical Issues

Santiago Candela-Cantó[1,2], Javier Aparicio[2], Jordi Muchart López[2,3], Pilar Baños-Carrasco[1,2], Alia Ramírez-Camacho[2], Alejandra Climent[2], Mariana Alamar[1,2], Cristina Jou[2,4], Jordi Rumià[1,2,5], Victoria San Antonio-Arce[2], Alexis Arzimanoglou[2,6], Enrique Ferrer [1,2,5]

Abstract

Stereoelectroencephalography (SEEG) is an effective technique to help to locate and to delimit the epileptogenic area and/or to define relationships with functional cortical areas. We intend to describe the surgical technique and verify the accuracy, safety, and effectiveness of robot-assisted SEEG in a newly created SEEG program in a pediatric center. We focus on the technical difficulties encountered at the early stages of this program. We prospectively collected SEEG indication, intraoperative events, accuracy calculated by fusion of postoperative CT with preoperative planning, complications, and usefulness of SEEG in terms of answering preimplantation hypothesis. Fourteen patients between the age of 5 and 18 years old (mean 10 years) with drug-resistant

Santiago Candela-Cantó (✉)
e-mail: scandela@sjdhospitalbarcelona.org
[1]Pediatric Neurosurgery Department, Sant Joan de Déu Barcelona Children's Hospital, Universitat de Barcelona, Passeig de Sant Joan de Déu 2, 08950 Esplugues de Llobregat, Barcelona, Spain
[2]Pediatric Epilepsy Surgery Unit, Sant Joan de Déu Barcelona Children's Hospital, Barcelona, Spain
[3]Diagnostic Imaging Department, Sant Joan de Déu Barcelona Children's Hospital, Universitat de Barcelona, Barcelona, Spain
[4]Pathology Department, Sant Joan de Déu Barcelona Children's Hospital, Universitat de Barcelona, Barcelona, Spain
[5]Neurosurgery Department, Hospital Clinic de Barcelona, Universitat de Barcelona, Barcelona, Spain
[6]Pediatric Epilepsy, Sleep and Neurophisiology Department, Centre Hospitalier Universitaire de Lyon and Hospital Femme-Mère-Enfant, Lyon, France

epilepsy were operated on between April 2016 and April 2018. One hundred sixty-four electrodes were implanted in total. The median entry point localization error (EPLE) was 1.57 mm (1–2.25 mm) and the median target point localization error (TPLE) was 1.77 mm (1.2–2.6 mm). We recorded seven intraoperative technical issues. Two patients suffered complications: meningitis without demonstrated germ in one patient and a right frontal hematoma in the other. In all cases, the SEEG was useful for the therapeutic decision-making. SEEG has been useful for decision-making in all our pediatric patients. The robotic arm is an accurate tool for the insertion of the deep electrodes. Nevertheless, it is an invasive technique not risk-free and many problems can appear at the beginning of a robotic arm-assisted SEEG program that must be taken into account beforehand.

Keywords Robotic arm, Frameless, Pediatric epilepsy surgery, Stereoelectroencephalography, Refractory epilepsy

Abbreviations

SEEG	Stereoelectroencephalography
EPLE	Entry point localization error
TPLE	Target point localization error
CT	Computed tomography
MRI	Magnetic resonance imaging
18F-FDG-PET	18 fluor-fluorodeoxyglucose-positron emission tomography
SPECT	Single positron emission computed tomography
fMRI	Functional magnetic resonance imaging
3 T	3 tesla
TFE	Turbo field echo
TOF	Time-of-flight
FLAIR	Fluid-attenuated inversion recovery
P-ICU	Pediatric intensive care unit
IQR	Interquartile range

Introduction

Stereoelectroencephalography (SEEG) was first described 56 years ago by Talairach and Bancaud [37]. Until two decades ago, the SEEG was systematically used in France and Italy for invasive presurgical evaluation in patients with refractory epilepsy, and only sporadically outside of these countries. However, nowadays an increasing number of epilepsy surgery centers around the world have started using this technique. Since 2015, our Multidisciplinary Pediatric Epilepsy Surgery Unit has evaluated about 125 children or adolescents with refractory epilepsy each year, of which in approximately 20% we have recommended epilepsy surgery and in 5% SEEG.

Stereoelectroencephalography has been proven as a safe and effective tool to help to locate and to delimitate the epileptogenic area and/or define relationships with functional cortical areas when this is not possible by noninvasive techniques in patients with focal drug-resistant epilepsy [5, 11, 19, 23, 32]. It allows epilepsy surgery teams to record electroencephalography in deep cortical structures and in bi-hemispheric explorations [35]. However, a so-called fishing expedition must be avoided and only few contralateral electrodes used to rule out a contralateral start just when considered necessary. In some cases, it is possible to thermocoagulate areas of the epileptogenic network with a therapeutic purpose [3]. Additionally, responsive close-loop neurostimulation is becoming clinically practiced [30].

The development of CT and MRI scanners in the 1970s was an important contribution to this technique [32], and it has become increasingly popular with the emergence of image-guided operative systems and neurosurgical robotics [6, 13, 16, 20, 27, 34, 35].

Only few papers refer exclusively to pediatric patients [9, 10, 12, 21, 26, 38, 39], in even fewer pediatric series, electrodes were implanted with a robotic arm [1, 12, 14, 24], and none of them refer to the technical problems they found at the beginning, neither to the robotic arm Neuromate®.

With the present study we aim to describe our initial experience with robot-assisted SEEG in terms of its accuracy and usefulness in an exclusively pediatric epilepsy surgery unit. We also focus on the intraoperative technical issues we found in the start-up of this program since April 2016.

Methods

Study design and Patient Selection

This is a 2-year prospective study on a cohort of pediatric patients affected by refractory epilepsy operated on SEEG to better localize the seizure onset zone or its functional relationships when noninvasive techniques were not enough to report this information.

Presurgical Evaluation

All patients underwent presurgical evaluation in our Multidisciplinary Pediatric Epilepsy Surgery Unit. The initial study included semiological analysis of seizures, interictal and ictal video-EEG, specific epilepsy MRI protocol, neuropsychological assessment according to patients' age, and nuclear medicine tests (18F-FDG-PET and/or SPECT) and motor and language fMRI in selected cases. In patients in whom noninvasive tests were not sufficient to define the epileptogenic area and/or its relationships with functional areas, SEEG was recommended.

Presurgical Plan

The presurgical imaging study for SEEG planning included a recent MRI and CT angiography examination, both within a month before the surgery. These studies were used to depict the

structural abnormalities, if present, and to best identify arterial and venous brain vessels for optimal presurgical planning and guidance.

Magnetic resonance imaging studies for presurgical evaluation were performed on a 3T MRI scanner Philips Ingenia (Philips Healthcare, Cleveland, Ohio, USA), with a 32-channel head-coil with the following sequences: sagittal T1 3D, TFE and TOF 3D, and sagittal T1 3D with contrast medium. Additional sequences were carried out according to the specific patient in case they could more easily depict structural lesions as seen on the patient's previous MRI studies.

The presurgical CT angiography was performed on a CT scanner Philips Brilliance iCT-256 (Philips Healthcare, Cleveland, OH, USA). Non-ionic contrast medium was administered in a by-phasic protocol to optimize both venous and arterial enhancement in a single CT acquisition [33].

Imaging datasets were loaded into the planning workstation with Voxim® software. CT angiography was defined as the referential set. MRI T1 3D TFE, TOF 3D, and additional MRI sequences (T2 3D or FLAIR 3D) when needed were merged to the CT angiography.

The different electrodes were planned according to the preimplantation hypotheses. Every electrode was checked and relocated to avoid vessels in CT angiography and TOF-sequence with a safety margin of 5 mm in diameter, while covering as much gray matter as possible in T1. The projection following the electrode axis was very useful for this purpose. Definitive trajectories were checked by at least three Epilepsy Surgery Unit members before being transferred to the robotic arm working station.

Surgical Technique

Electrode placement was assisted by the robotic arm Neuromate® (Renishaw®).

Surgery was held under general anesthesia and cefazolin antibiotic prophylaxis (one preoperative dose and three postoperative doses). The accuracy of the robotic arm was calibrated before every single procedure. After this, the fiducial support and three parasagittal screws of 25 mm (Dixi Medical ACS-025SMS-10) were fixed to the patient's skull as surface EEG reference points and to verify intraoperative accuracy (Fig. 1a).

For stereotactic spatial patient registration, a preoperative CT was acquired with a fiducial reference fixed to the patient's skull (Fig. 1b). The referenced CT was co-registered to the preoperative angio-CT containing the planned trajectories and they were transferred to the new intraoperative CT using the Voxim® software. The patient's head was stabilized with the six-pin robotic arm head-holder. No stereotactic frame was employed. The co-registration was based on fiducial recognition and location through ultrasounds (Fig. 1c).

We checked accuracy localizing surface screws with the laser pointer (Fig. 1d, e).

In the first two patients, we shaved the whole head, but in the rest of the patients, we preferred to shave only the entry points. So, before inserting the electrodes, we checked all trajectories over the patient's head and shaved an area of 1 cm^2 around every entry point (Fig. 1f).

After draping the surgical field, the robotic arm positioned itself into the trajectory to insert the electrodes. For each electrode, we incised the skin with a punch (Dixi Medical ACS745), coagulated skin with a blunt tipped electrode (Dixi Medical KIP-ACS-605), and drilled with a 2.5-mm

Fig. 1: a Fiducial support screwed to patient's skull and surface screws for surface EEG and accuracy check. **b** CT with fiducial attached to patient's head. **c** Ultrasound location for coregistration. **d** and **e** Accuracy check localizing surface screws with the laser tool. **f** Trajectories check and minimal shaving. **g** Hand chisel for calculation of the length of the drill. **h** Dura mater coagulation. **i** Carving the electrode path with a stylet. **j** Electrode length measurement. **k** and **l** Electrodes wrapping.

drill (Dixi Medical KIP-ACS-515). The length of the drill was calculated according to the thickness of the bone in the preoperative CT and measured with a hand chisel [Medicon 27-57-(4-12)] (Fig. 1g). Dura mater was coagulated and opened with a sharp-tipped coagulating stylet (Dixi Medical KIP-ACS-600) (Fig. 1h).

The bone screw was inserted through the 2.5-mm guide (provided by Renishaw®) and the distance between the robot and the screw was measured with a flat tip thick stylet (Dixi Medical ACS-740). We subtracted this distance from the robot-to-target distance to obtain the screw-to-target length. We carved the intraparenchymal trajectory with a thin stylet (Dixi Medical ACS-770S-10) (Fig. 1i) and then replaced it with the electrode [Dixi Medical D08-(05-18)] to the calculated depth (Fig. 1j). The stylet was kept in place until it was replaced by the electrode to prevent unnecessary CSF leakage. Once all electrodes were inserted, a postoperative CT (still under general anesthesia) was performed in order to rule out intraoperative complications and to check accuracy.

After this, we removed the fiducial screw and wrapped the patient's head and secured the electrodes (Fig. 1k, l). The patient was awakened from anesthesia in the operating room and transferred to the pediatric intensive care unit (P-ICU).

The surgical technique is shown in Video 1.

Postsurgical Evaluation

Postsurgical imaging was performed on a 1.5T MRI scanner (Signa General Electric, Milwaukee, USA) because of MRI safety restrictions according to the SEEG electrode vendor (Dixi Medical)—currently not approved for 3 T. Postoperative MRI included an axial FSPGR 3D BRAVO and

sagittal CUBE T2. Afterwards, the patient was transferred to the Pediatric Epilepsy Surgery Unit for continuous video-SEEG monitoring.

Accuracy

We determined accuracy of the system by calculating the distances between the electrodes and their respective planned trajectories at the entry point (EPLE, entry point localization error) as well as at the target point (TPLE, target point localization error). To do so, we merged the post-operative CT with the preoperative plan using the Voxim® software and the measuring tools provided by this software as shown previously elsewhere [4].

Surgical Duration, Intraoperative Events, and Complications

Surgical duration, intraoperative events, and complications were recorded.

Utility Assessment

The most important goal was whether SEEG in our hands was useful or not for making therapeutic decisions: delimiting the seizure onset zone, defining the relationship with functional areas, or providing any other clinical information that would not have been possible without this technique [25].

Results

Demographic Aspects

We have operated on 14 patients affected by refractory epilepsy aged 5 to 18 years old (mean 10 years), between April 2016 and April 2018.

Table 1 summarizes demographic, clinical data, and SEEG indication.

Electrodes and Accuracy

We have inserted 9–15 electrodes/patient, 164 electrodes in total. EPLE was of 1.57 mm (1–2.25 mm) and TPLE of 1.77 mm (1.2–2.6 mm). Accuracy for every patient is described in Table 2.

Surgical Duration and Intraoperative Events

Mean surgical duration was 6 h 54' (5 h 10'–8 h 5').

Several issues contributed to this long operative time.

We had to relocate the head-holder in patient 5 because of coinciding with temporal posterior trajectories.

Table 1: Summary of demographic data of the patients. *R*, right; *L*, left; *F*, frontal; *Fb*, frontobasal; *P*, parietal; *T*, temporal; *Tb*, temporal basal; *O*, occipital; *I*, insular; *a*, anterior; *p*, posterior; *s*, superior; *m*, mesial; *SMA*, supplementary motor area; *NL*, non lesional; *FCD*, focal cortical dysplasia; ?, doubtful

Patient	Age SEEG (years)	Epilepsy onset	Seizure type* All focal onset	MR	Localization Hypothesis‡	Indication†
1	9	3 days	Tonic + impaired awareness ± hyperkinetic or autonomic	R-T a m residual tumor + R-Fb porencephaly	1. R-T a m 2. R-I a s 3. R-Fb	1, 2
2	9	4 years	Asymmetric tonic + hyperkinetic + impaired awareness	Suspected R-F superior sulcus FCD	R-F ± P	1, 3
3	18	15 years	L-crural somatosensory aura → tonic + clonic	NL (R-central PET hypometabolism)	R-Primary Motor	1, 3
4	17	12 years	± Auditive aura → impaired awareness ± myoclonic/clonic → tonic	NL (bilateral temporal PET hypometabolism)	1. L-I p 2. L-Tb 3. L-FTI	1, 2, 3
5	5	7 months	± Impaired awareness ± automatisms ± L-clonic ± autonomic	R-hemisphere atrophy (mainly posterior) Perinatal infarct?	R-TPO	1, 3
6	16	7 years	Dizziness aura → ± impaired awareness → ± hyperkinetic/ automatisms → ± bilateral tonic-clonic	Bilateral centroparietal polymicrogyria + schizencephaly	1. R-P 2. Bilateral	1, 2, 3
7	15	3 years	Impaired awareness → L-braquial tonic ± L-hand and oral automatisms	L-Tb and a FCD and L-Fb FCD?	L-Tb and a ± Fb	1, 3
8	7	6 months	Psiquic aura → hyperkinetic → L-tonic	R-T a m tumor + FCD	R-T ± I	1
9	9	5 years	± Somatosensory aura → asymmetric tonic → clonic	R-F premotor FCD	R-premotor ± motor	1, 3, 4$^{\$}$
10	5	5 months	Myoclonic or tonic or spasms	Postsurgical residual R-FbTI FCD?	R-FbTI	1, 3
11	7	5 years	Epigastric aura → ± automatisms ± impaired awareness	L-T pole ± fusiform gyrus FCD ± hippocampal sclerosis	L-T pole ± fusiform gyrus ± hippocampus	1, 3
12	5	2 years	Automotor + impaired awareness	R-anterior cingulum FCD?	R-cingulum ± FTI	1
13	13	6 months	Somatosensory aura ± spasms	L-F FCD	L-F	1, 3
14	10	16 months	Asymmetric tonic	NL (R-I PET hypometabolism)	1. R-F SMA 2. R-I	1, 2, 3
Mean	10	4 years				

*According to ILAE operational classification of seizure types of 2017 [17]
‡Localization hypothesis listed from most to least probable according to previous studies
†From Jayakar *et al.* [25]: 1—to define the EZ (epileptogenic zone) precisely when noninvasive data are inconclusive; 2—to resolve divergence of noninvasive data pointing to two or more regions; 3—to map eloquent cortical function precisely; 4—secondary indications (thermocoagulation)
$^{\$}$Thermocoagulation was indicated after analyzing the SEEG register and after electrical stimulation

Table 2: Implantation plan, precision, and complications. *R*, right; *L*, left; *B*, bilateral; *F*, frontal; *P*, parietal; *T*, temporal; *O*, occipital; *I*, insular; *EPLE*, entry point localization error; *TPLE*, target point localization error; *IQR*, interquartile range

Patient	Implantation plan	Num. electrodes	EPE mm (IQR)	TPE mm (IQR)	Surgical time	Intraoperative incidences/ complications
1	R-FTI	10	1.75 (1.42–2)	1.5 (1.42–2.4)	7 h 45'	Electrodes' collision
2	R-F	9	1.9 (1.5–2)	1 (0.5–1.4)	7 h	Electrodes' collision Electrode cap breakage
3	R-Central	9	0.5 (0.5–0.8)	1.2 (0.8–1.8)	7 h	Marker search error
4	L-FTI	15	0.55 (0.5–0.95)	1.8 (1.5–2.05)	7 h 10'	Meningitis
5	R-PTOI	12	1.3 (0.95–1.75)	1.35 (0.77–1.75)	7 h 25'	Head-holder relocation
6	B-FPI	14	2 (1.72–2.5)	1.27 (0.97–2)	7 h 50'	
7	L-FTI	12	2.17 (1.45–2.47)	1.65 (0.97–2.67)	8 h 5'	
8	R-FTPI	12	1.47 (1.33–2.2)	1.65 (1.41–2.65)	8 h	Temporal pole (PT) electrode not possible
9	R-FP	11	1.55 (1.37–1.67)	1.85 (1.7–1.92)	7 h 55'	
10	R-FTI	10	1.82 (1.65–2.18)	2.35 (2.16–2.75)	6 h 15'	
11	L-T	10	3.12 (2.91–3.3)	3.05 (2.63–3.83)	5 h 45'	
12	R-FTI	13	3.1 (2.75–3.3)	3.65 (3.15–4.2)	5 h 20'	Hematoma
13	R-FT	14	0.75 (0.64–1.07)	1.38 (1.17–1.83)	6 h 5'	Fiducial screw in coronal suture Collision electrode caps
14	R-FI	13	1.07 (0.9–1.4)	1.4 (0.75–1.85)	5 h 10'	Collision electrode caps Surface screw coincidence Electrodes' collision
Mean		11.7	1.57 (1–2.25)	1.77 (1.2–2.6)	6 h 54'	

In patient 13, the fiducial screw was inserted in the coronal suture (Fig. 2a). When we changed the CT fiducial for the ultrasounds' microphone for registration, the screw loosened, and we had to screw it deeper and repeat the CT.

In the third patient, we selected the fiducial support instead of the fiducials themselves in the "marker search" step. This support has a similar shape when seen on the CT but different density (Fig. 2b, c). When we checked the precision on the surface screws we realized that there was an error of 10 mm in depth. Voxim® did not detect the mistake because fiducials and their support have the same geometry.

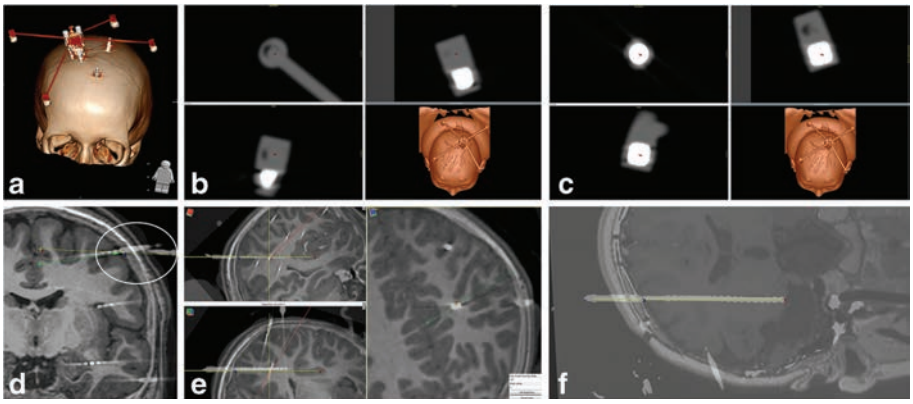

Fig. 2: a Fiducial screw inserted in the coronal suture. **b** Selection of fiducial support instead of the fiducials themselves in the "marker search step" (wrong). **c** Fiducial selection in the "marker search step" (right). Fiducials are more dense than their support. **d** Electrode caps collision. **e** Electrodes collision. **f** Transfrontal trajectory to the amygdala to avoid postsurgical porencephaly.

In patient 8 (7 years old), the bone screw was not stable enough to insert the electrode in the temporal pole, so its placement was declined.

In patients 13 and 14, two entry points were very close and the electrode caps collided (Fig. 2d). It was solved using screws of different lengths.

In patients 1, 2, and 14, two electrodes collided in their trajectories (Fig. 2e). In two cases, we felt some resistance when inserting the second electrode. In the other case, we realized it after the postoperative CT. TPLE in these patients was 1.875 (1.25-2.75).

In the postoperative CT of patient 2, we also detected an electrode that was 13 mm shallower than planned. It was due to electrode cap breakage. We had to replace and reinsert this electrode to the adequate depth.

Neurophysiologic Recording

After spending the first postoperative night in the P-ICU, the postoperative MRI was performed, and the patients were transferred to the epilepsy unit for continuous monitoring.

The electrodes were maintained between 3 and 17 days (8.8 days on average). Patient 4 required implantation of an additional electrode the fifth day of SEEG monitoring. Electrodes were maintained for 17 days in this patient.

Electrical stimulation and brain mapping were performed in all patients, except patient 12. In those patients in whom dominant hemisphere for language was explored, nomination, repetition, and comprehension were meticulously evaluated.

Patients were discharged 1 or 2 days after explantation.

Data recorded were analyzed and the treatment plan was decided in the Multidisciplinary Epilepsy Unit Board.

Complications of SEEG

Two patients suffered complications of clinical significance.

Patient 4 suffered a meningitis without a demonstrated germ. He required a 17-day implantation including a second reimplantation to determine more precisely the ictal onset. Immediately after removing the electrodes, he presented with dysphasia and right mydriasis and ophthalmoplegia due to cranial nerve III palsy. Brain MRI showed meningeal enhancement after contrast administration at the left temporal implantation area and at the right tentorial cleft (Fig. 3a, b). The patient remained without a fever and did not present a significant alteration of the acute phase reactants in blood. The CSF obtained by lumbar puncture was compatible with aseptic or aborted meningitis. Antibiotic therapy and corticosteroids were administered according to normal protocol with good clinical and radiological response.

Patient 12 suffered a right frontal hematoma. It was not visible in the postoperative CT but appeared in the MRI performed 19 h after the surgery (Fig. 3c). The patient remained clinically stable during 3 days and neurophysiological monitoring was allowed, but on the 3rd day, surgical evacuation was required and a resective surgery was also intended with the partial information obtained in SEEG monitoring.

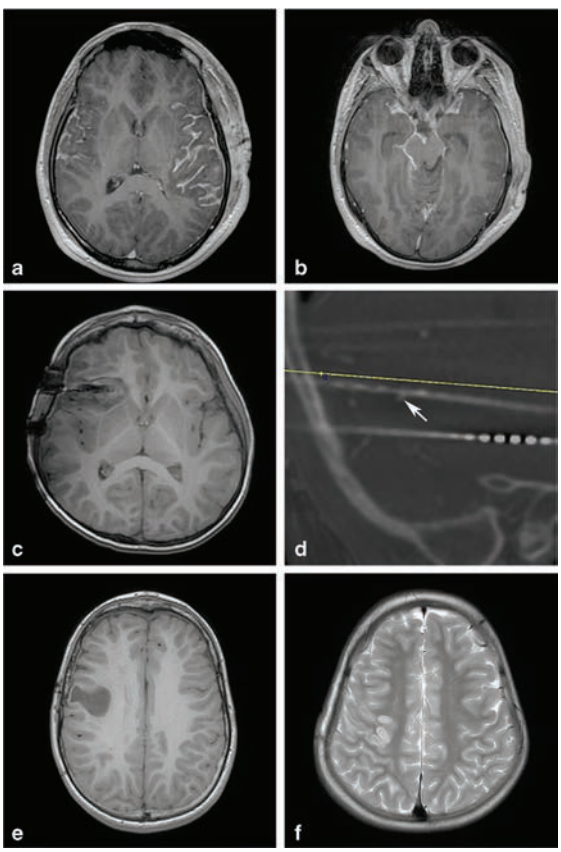

Fig. 3: a MRI T1 showing meningeal enhancement at the left temporal implantation area due to meningitis. **b** MRI T1 showing meningeal enhancement at the right tentorial cleft due to meningitis. **c** MRI T1 showing a right frontal hematoma 19 h after the implantation. **d** Electrode displacement towards mid cerebral artery branch (*arrow*) causing a hematoma seen on postoperative CT fused with preoperative plan. **e** Asymptomatic venous infarct seen in MRI T1. **f** MRI T2 showing radiologic findings after thermocoagulation.

Four small foci of cortico-subcortical bleeding with edema were detected in post-explant MRI in different patients. They could be related to small venous infarcts due to dural coagulation. None of them had clinical repercussions (Fig. 3e).

Usefulness of SEEG

In all cases, the SEEG was useful for making the therapeutic decision, and preimplantation enquiries were answered in 12 of the 14 patients.

In patient 12, one of the preimplantation hypotheses included anterior cingulum. This patient suffered a hematoma that prevented us from exploring this area.

In patient 13, ictal onset was not well defined. Information obtained with the SEEG allowed us to delimitate the epileptogenic zone ahead of the central sulcus, but we could not discard motor cortex involvement in epilepsy onset.

Surgery was disregarded in two patients, in one by overlapping of the ictal onset with the primary motor and sensory area and in the other by multiple ictal initiations related to language eloquent cortex.

In 10 patients, resective or disconective surgery was decided. Thermocoagulation was performed in one (Fig. 3f) after evaluating SEEG register and stimulation, but it was not effective enough and the patient underwent resective surgery.

Two more patients are waiting for the operation.

Discussion

Stereoelectroencephalography is a safe and effective technique in difficult-to-localize epilepsy [5, 35]. Its safety depends, in part, on the technique chosen for electrode implantation and on a careful preimplantation plan. Moreover, proper preimplantation hypothesis and data analysis are crucial for effectiveness.

In this paper, we report our initial experience with the use of the robotic arm to insert SEEG depth electrodes for difficult-to-localize epilepsy in pediatric patients. SEEG was recommended in a small part of our candidates for epilepsy surgery. This is due to the fact that patients with developmental tumors (frequently associated to FCD) or those with multilobar or hemispheric malformations, so frequent in pediatrics, rarely need an invasive exploration. Since we started our SEEG program, we no longer perform invasive monitoring with subdural grids as in our experience, SEEG is better tolerated in children. This is probably due to their lower tolerance to swelling related to their higher brain volume compared to their skull capacity. However, we do not rule out this technique for future selected cases.

There are some particularities when using the stereotactic robot for SEEG in the pediatric population that must be underlined. First point is that children are more sensitive to radiation exposure. At least three CT scans are needed in the technique described. Despite that they are done with a pediatric low radiation protocol, it is desirable to reduce them. The preoperative by-phasic CT angiography [33] provides less radiation than an angiography. Besides that, Neurolocate® (a

new version of the Neuromate® software) will allow to perform the registration process with only two radiographs, sparing one of the CT scans. Finally, the postoperative CT scan is important to rule out intraoperative complications and allows us to locate the electrodes precisely when merging it with the preoperative MRI. It could be replaced by an MRI, but we prefer to perform the MRI as a deferred exploration 24 h postoperative to watch out delayed problems and to obtain additional information about electrode location. Arranging the MRI just after the surgery in our hospital is currently difficult.

Second point refers to bone thickness. Children have a bone thinner than adults, especially in younger ages. We checked bone thickness preoperatively for every trajectory. In some cases, we needed to change the desired trajectory to avoid postsurgical bone defects or areas with skull thinner than 2 mm, specifically in the temporal region in younger children. In fact, in patient 8 (7 years old), we were not able to insert a temporal electrode because the screw was not stable enough. In this case, the thickness of the bone was of 3 mm, the trajectory was oblique, and the screw suffered displacements by the temporal muscle contractions. In our series, the younger patients were 5 years of age and the minimum bone thickness of 3 mm. This is a relatively common limit usually corresponding to children older than 3 years, but Taussig *et al*. describe the feasibility of this exploration in children as young as 5 months. Anyway, they recognize that in children younger than 2 years old, cranial and electrode fixation limit this technique [38].

Third, the cerebral cortex is also thinner in younger patients. This makes it often difficult to place the minimum of two contacts in the cortex maintaining the safe distance from vessels.

Finally, the degree of collaboration in younger patients during monitoring is limited. For this reason, we assure the electrodes with a capelin as shown in Fig. 1k, l.

We have recorded several intraoperative events; however, only two of them were of clinical significance, and none has left permanent neurological deficits. We consider most of these related to the learning curve associated with starting a new technique in our hospital. For this reason, we describe them in detail to help other neurosurgical teams to avoid them in their first robot-assisted surgeries. In our opinion, all these events also contributed to lengthen the surgical time.

In patients in whom resective surgery failed and a SEEG was proposed, bone and porencephaly cavities have to be checked. In the first patient, we had to reach the amygdalar nucleus from the frontal lobe to avoid a temporal postsurgical cavity (Fig. 2f). Alternatively, we also could have used an electrode with an inner wire stylet (Ad-tech Medical).

Checking the preoperative 3D reconstruction with the trajectories while stabilizing the patient's head can help to avoid having to relocate the head-holder. It is also recommended to avoid the coronal suture when inserting the fiducial screw.

In the "marker search" step of patient registration of the robotic arm software, attention must be paid to select the fiducials (of higher radiopacity) and not their support (Fig. 2b, c). Their shapes are similar, and their geometry is identical, so they could be mistaken, and the system would not detect this mistake if an accuracy check was not made after registration. It is of great importance to check precision with surface screws to rule out errors during registration.

In case of excessive closeness of two trajectories at the entry point, it can be solved using screws of different lengths.

Collision of electrodes along their trajectories should be avoided. It could cause its deviation. We did not find significant differences in TPLE in the trajectories that collided. Even so, attention should be paid when planning and revising the trajectories in the 3D reconstruction of the planning software. A safety margin of 1 cm between electrodes at their entry point and along their trajectory has been recommended [24]. If any resistance was felt while introducing the electrode, this maneuver should be stopped and trajectories should be checked once more. Teams using exclusively orthogonal implantation trajectories seldom experience this issue. The collision of trajectories in three patients despite a meticulous planning might reflect limitations in the planning software. Dixi Medical has improved the design of the cap doing its breakage more difficult.

Finally, difficulties in transferring postoperative CT datasets for its co-registration with preplanned trajectories for postoperative accuracy check also contributed to the lengthened surgical time. An intraoperative CT [1] or MRI [34] or connecting the robotic arm via network would solve this problem. Increasing surgical expertise can also help to reduce surgical time. In fact, it has evolved from more than 8 h in the first patient to 5 h in the last one, with a mean time for electrode of less than 10 min in this case.

The accuracy obtained in our procedures (EPLE of 1.57 mm and TPLE of 1.77 mm) was similar to that reported by other groups with other frameless stereotaxic systems (EPLE 0.86–2.53 mm and TPLE 1.7–2.96) [2, 6, 8, 14, 18, 22, 28, 36, 41] and to frame-based systems (EPLE 1.54 and TPLE 1.1–2.93) [19, 40]. See Table 3. Leaving a "safety cylinder" of 5 mm in diameter around each trajectory is coherent with our interquartile range (EPLE 1.57–2.25 mm and TPLE 1.2–2.6 mm). Accuracy for our DBS procedures has been described elsewhere [3].

We have detected that the accuracy of the robotic system may diminish over time and after several procedures. We also noticed a significant improvement of the accuracy after every maintenance of the robotic arm (Fig. 4). This could be related to moving the robot in and out of the operating room before and after its use. Therefore, it is extremely important to perform the scheduled maintenance, to not move the robot out of the operating room and to check accuracy before and after every surgery.

We suffered two major complications in our short series: a meningitis and a hemorrhage. These are the most common complications described in the literature [13, 22, 29, 31]. None of these patients had permanent neurological impairment.

The patient affected by the meningitis required a long implantation including a reimplantation. These are the most important risk factors for infection in these patients, apart from CSF leak. SEEG monitoring time must be as short as possible to respond to preimplantation hypothesis. There is no evidence that not shaving the entire head increases the risk of infection. Our patients are able to return to school 2 days after explantation so their appearance and social environment has to be taken into account and we prefer not to shave.

The hematoma was related to a misplaced electrode to anterior cingulum. Accuracy of this electrode was of 3.3 mm at the entry point and 4.55 mm at the target point. Accuracy in this patient had a median of 3.1 mm (IQR 2.75–3.3 mm) at the entry point and 3.65 mm (IQR 3.15–4.2) at the target point. Frontal lobe implantation has been related to an increased risk of bleeding [13, 38]. In our opinion, loss of accuracy contributed to this hematoma as the electrode was

Table 3: Accuracy in different series with different stereotactic systems (based on Van der Loo *et al*. [40]). *P*, pediatric patients; *A*, adult patients; *Ph*, phantom; -, not specified; *EPLE*, entry point localization error; *TPLE*, target point localization error

Study	Year	Patients	Stereotactic system	Trajectories	EPLE (mm)	TPLE (mm)
Golash A *et al*. [18]	2000	Ph	Neuromate®		2.4	
Li *et al*. [28]	2002	Ph	Neuromate® robot	5	1.95	
Cardinale *et al*. [6]	2013	A + P	Talairach frame	517	1.43	2.69
			Neuromate® robot	1050	0.78	1.77
González-Martínez *et al*. [19]	2013	A + P	Leksell® frame	1367		1.1
Balanescu *et al*. [2]	2014	A	StarFix® 3D printed	52	0.68	1.64
González-Martínez *et al*. [20]	2016	A + P	Rosa® robot	500	1.2	1.7
Verburg *et al*. [41]	2016	A + P	Varioguide®	89		3.5
Roessler *et al*. [34]	2016	A	Intraoperative MRI navigated tube	58	3.2	1.4
Cardinale *et al*. [8]	2017	Ph	Neuromate® Neurolocate	40	0.59	1.49
		-	Neuromate®	127	0.78	1.77
De Benedictis *et al*. [14]	2017	P	Rosa® robot	386	1.5	1.96
Van der Loo *et al*. [40]	2017	A + P	Leksell® frame	854	1.54	2.93
Dorfer *et al*. [16]	2016	A + P	iSys1 robot	93	1.3	1.5
Spyrantis *et al*. [36]	2018	A	Rosa® robot with MRI registration	40	2.53	2.96
Present report	2018	P	Neuromate	164	1.57	1.77

misplaced towards a branch of the middle cerebral artery (Fig. 3d). This hematoma was not shown in immediate postoperative CT, rather in the MR performed 19 h after the surgery. Delayed occurrence of a hematoma after SEEG has already been described [15], so a deferred neuroimaging exploration should not be obviated.

Cerebral angiography can be useful to decrease the risk of hemorrhage [7, 22]. The most experienced SEEG groups have incorporated it to their standard practice. We perform a double-contrast CT [33] instead of the angiography. In our short experience, this technique is also useful for this purpose. In our patient, the problem was not in the preoperative plan, rather in the accuracy of the robot. In fact, EPLE and TPLE in the previously operated patient were of 3.12 mm and 3.37 mm respectively. In Fig. 4, it is shown that the risk of bleeding could be related to accuracy

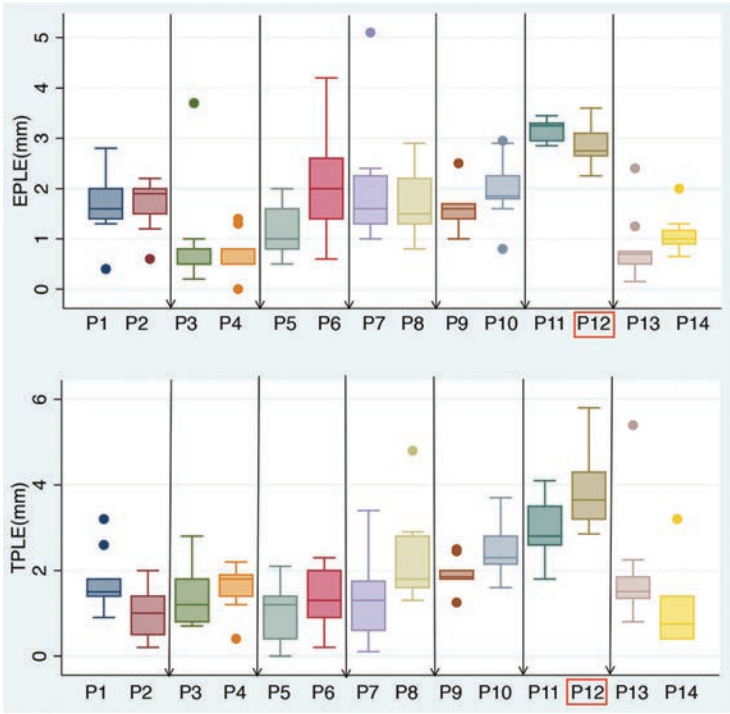

Fig. 4: Diagram of accuracy for every patient at the entry point defined as the entry point localizing error (EPLE) (*up*) and at the target point as the target point localizing error (TPLE) (*down*) calculated with STATA14. *Vertical arrows* indicate when the robot maintenance was held. The *red square* highlights the patient who suffered a hematoma.

worsening. Accuracy must be checked not only before every surgery but also after every operation too and, in case of detecting an incipient impairment, a robot maintenance is mandatory.

Stereoelectroencephalography answered the questions posed by the preimplantation hypotheses for almost all our patients and was useful for therapeutic decision in all cases. Epilepsy surgery outcome will be reported when longer follow-up is reached.

Conclusions

Stereoelectroencephalography has been useful for decision-making in our pediatric patients. The robotic arm is an accurate tool for the insertion of the deep electrodes. Nevertheless, this is a complex and invasive procedure. Thus, it is not risk-free and many issues may arise at the beginning of a robotic-assisted SEEG program that has to be taken into account beforehand.

Acknowledgments We thank Carles Fàbrega and Gemma Fernandez for helping us with video editing. We thank Matthew Ponticiello for reviewing the English.

Compliance with ethical standards

Conflict of interest The authors declare that they have no conflict of interest.

Ethical approval All surgeries were part of standard patient care and not for research purposes. All procedures performed were in accordance with the 1964 Helsinki Declaration and its later amendments or comparable ethical standards. The study was approved by the Research and Ethics committee of Sant Joan de Déu Barcelona Hospital.

Informed consent Informed consent was obtained from all individual participants included in the study or their legal guardians.

References

1. Abel TJ, Varela Osorio R, Amorim-Leite R, Mathieu F, Kahane P, Minotti L, Hoffmann D, Chabardes S (2018) Frameless robotassisted stereoelectroencephalography in children: technical aspects and comparison with Talairach frame technique. J Neurosurg Pediatr 22:37–46.
2. Balanescu B, Franklin R, Ciurea J, Mindruta I, Rasina A, Bubulescu RC (2014) A personalized stereotactic fixture for implantation of depth electrodes in stereoelectroencephalography. Stereotact Funct Neurosurg 92:117–125.
3. Bourdillon P, Debaux P, Job-Chapron AS, Isnard J (2018) SEEG-guided radiofrequency thermocoagulation. Neurophysiol Clin 48: 59–64.
4. Candela S, Vanegas M, Darling A, Ortigoza-Escobar D, Alamar, Muchart J, Climent A, Ferrer E, Rumià J, Pérez-Dueñas B (2018) Frameless robot-assisted pallidal deep brain stimulation in pediatric patients for movement disorders: precision and short-term clinical results. J Neurosurg Pediatr 22:416–425. https://doi.org/10.3171/ 2018.5.PEDS1814
5. Cardinale F, Casaceli G, Raneri F, Miller J, Lo Russo G (2016) Implantation of stereoelectroencephalography electrodes: a systematic review. J Clin Neurophysiol 33:490–502.
6. Cardinale F, Cossu M, Castana L, Casaceli G, Schiariti MP, Miserocchi A, Fuschillo D, Moscato A, Caborni C, Arnulfo G, Lo Russo G (2013) Stereoelectroencephalography: surgical methodology, safety, and stereotactic application accuracy in 500 procedures. Neurosurgery 72:353–366.
7. Cardinale F, Pero G, Quilici L, Piano M, Colombo P, Moscato A, Castana L, Casaceli G, Fuschillo D, Gennari L, Cenzato M, Lo Russo G, Cossu M (2015) Cerebral angiography for multimodal surgical planning in epilepsy surgery: description of a new three-dimensional technique and literature review. World Neurosurg 84: 358–367.
8. Cardinale F, Rizzi M, d'Orio P, Casaceli G, Arnulfo G, Narizzano M, Scorza D, De Momi E, Nichelatti M, Redaelli D, Sberna M, Moscato A, Castana L (2017) A new tool for touch-free patient registration for robot-assisted intracranial surgery: application accuracy from a phantom study and a retrospective surgical series. Neurosurg Focus 42:E8.
9. Cossu M, Cardinale F, Castana L, Nobili L, Sartori I, Lo Russo G (2006) Stereo-EEG in children. Childs Nerv Syst 22:766–778.
10. Cossu M, Cardinale F, Colombo N, Mai R, Nobili L, Sartori I (2005) Stereoelectroencephalography in the presurgical evaluation of children with drug-resistant focal epilepsy. J Neurosurg Pediatr 103(Suppl 4):333–343.
11. Cossu M, Chabardes S, Hoffmann D, Russo G (2008) Explorations préchirurgicales des épilepsies pharmacorésistantes par stéréoélectro-encéphalographie: principes, technique et complications. Neurochirurgie 54:367–373.
12. Cossu M, Schiariti M, Francione S, Fuschillo D, Gozzo F, Nobili L, Cardinale F, Castana L, Lo Russo G (2012) Stereoelectroencephalography in the presurgical evaluation of focal epilepsy in infancy and early childhood. Clinical article. J Neurosurg Pediatr 9:290–300.
13. De Almeida AN, Olivier A, Quesney F, Dubeau F, Savard G, Andermann F (2006) Efficacy of and morbidity associated with stereoelectroencephalography using computerized tomography-or magnetic resonance imaging-guided electrode implantation. J Neurosurg 104:483–487.
14. De Benedictis A, Trezza A, Carai A, Genovese A, Procaccini E, Messina R, Randi F, Cossu S, Esposito G, Palma P, Amante P, Rizzi M, Marras CE (2017) Robot-assisted procedures in pediatric neurosurgery. Neurosurg Focus 42:2–12.
15. Derrey S, Lebas A, Parain D, Baray MG, Marguet C, Fregue P, Proust F (2012) Delayed intracranial hematoma following stereoelectroencephalography for intractable epilepsy: case report. J Neurosurg Pediatr 10:525–528.
16. Dorfer C, Minchev G, Czech T, Stefanits H, Feucht M, Pataraia E, Baumgartner C, Kronreif G, Wolfsberger S (2016) A novel miniature robotic device for frameless implantation of depth electrodes in refractory epilepsy. J Neurosurg 126:1622–1628.
17. Fisher RS, Cross JH, French JA, Higurashi N, Hirsch E, Jansen FE, Lagae L, Moshé SL, Peltola J, Perez ER, Scheffer IE, Zuberi SM (2017) Operational classification of seizure types by the International League Against Epilepsy: position paper of the ILAE Commission for Classification and Terminology. Epilepsia 58:522–530.
18. Golash A, Eldridge PR, Varma TRK, Byrnel P, Badano F, Nahum B, Pittet P (2000) 3-D error measurement for checking the application accuracy of a stereotactic robotic system with an infrared space digitisation technique: a phantom study and clinical use. Acta Neurochir 142:1169–1210.
19. González-Martínez J, Bulacio J, Alexopoulos A, Jehi L, Bingaman W, Najm I (2013) Stereoelectroencephalography in the "difficult to localize" refractory focal epilepsy: early experience from a North American epilepsy center. Epilepsia 54:323–330.
20. González-Martínez J, Bulacio J, Thompson S, Gale J, Smithason S, Najm I, Bingaman W (2016) Technique, results and complications related to robot-assisted stereoelectroencephalography. Neurosurgery 78:169–180.
21. Gonzalez-Martínez J, Mullin J, Bulacio J, Gupta A, Enatsu R, Najm I, Bingaman W, Wyllie E, Lachhwani D (2014) Stereoelectroencephalography in children and adolescents with difficult-to-localize refractory focal epilepsy. Neurosurgery 75(3):258–268.
22. González-Martínez J, Mullin J, Vadera S, Bulacio J, Hughes G, Jones S, Enatsu R, Najm I (2014) Stereotactic placement of depth electrodes in medically intractable epilepsy. J Neurosurg 120:639– 644.
23. Guenot M, Isnard J, Ryvlin P, Fischer C, Ostrowsky K, Mauguiere F, Sindou M (2001) Neurophysiological monitoring for epilepsy surgery: the Talairach SEEG method. Indications, results, complications and therapeutic applications in a series of 100 consecutive cases. Stereotact Funct Neurosurg 77:29–32.

24. Ho AL, Muftuoglu Y, Pendharkar AV, Sussman ES, Porter BE, Halpern CH, Grant GA (2018) J Neurosurg Pediatr. https://doi.org/10.3171/2018.5.PEDS17718
25. Jayakar P, Gotman J, Harvey AS, Palmini A, Tassi L, Schomer D, Dubeau F, Bartolomei F, Yu A, Kršek P, Velis D, Kahane P (2016) Diagnostic utility of invasive EEG for epilepsy surgery: indications, modalities, and techniques. Epilepsia 57:1735–1747.
26. Kim H, Lee C, Knowlton R, Rozzelle C, Blount JP (2011) Safety and utility of supplemental depth electrodes for localizing the ictal onset zone in pediatric neocortical epilepsy. J Neurosurg Pediatr 8: 49–56.
27. Kwoh YS, Hou J, Jonckheere EA, Hayati S (1988) A robot with improved absolute positioning accuracy for CT guided stereotactic brain surgery. IEEE Trans Biomed Eng 35:153–160.
28. Li QH, Zamorano L, Pandya A, Perez R, Gong J, Diaz F (2002) The application accuracy of the NeuroMate robot—a quantitative comparison with frameless and frame-based surgical localization systems. Comput Aided Surg 7:90–98.
29. McGonigal A, Bartolomei F, Régis J, Guye M, Gavaret M, Trébuchon-Da Fonseca A, Dufour H, Figarella-Branger D, Girard N, Péragut JC, Chauvel P (2007) Stereoelectroencephalography in presurgical assessment of MR-negative epilepsy. Brain 130:3169–3183.
30. McGovern RA, Alomar S, Bingaman WE, Gonzalez-Martinez J (2018) Robot-assisted responsive neurostimulator system placement in medically intractable epilepsy: instrumentation and technique. Oper Neurosurg (Hagerstown). https://doi.org/10.1093/ons/opy112
31. Mullin JP, Shriver M, Alomar S, Najm I, Bulacio J, Chauvel P, Gonzalez-Martinez J (2016) Is SEEG safe? A systematic review and meta-analysis of stereo-electroencephalography-related complications. Epilepsia 57:386–401.
32. Munari C, Hoffmann D, Francione S, Kahane P, Tassi L, Lo Russo G, Benabid AL (1994) Stereo-electroencephalography methodology: advantages and limits. Acta Neurol Scand Suppl 152:56–69.
33. Rodallec MH, Krainik A, Feydy A, Hélias A, Colombani JM, Jullès MC, Marteau V, Zins M (2006) Cerebral venous thrombosis and multidetector CT angiography: tips and tricks. Radiographics 26(Suppl 2):S5–S18.
34. Roessler K, Sommer B, Merkel A, Rampp S, Gollwitzer S, Hamer HM, Buchfelder M (2016) A frameless stereotactic implantation technique for depth electrodes in refractory epilepsy utilizing intraoperative MR imaging. World Neurosurg 94:206–210.
35. Serletis D, Bulacio J, Bingaman W, Najm I, González-Martínez J (2014) The stereotactic approach for mapping epileptic networks: a prospective study of 200 patients. J Neurosurg 121: 1239–1246.
36. Spyrantis A, Cattani A, Strzelczyk A, Rosenow F, Seifert V, Freiman TM (2018) Robot-guided stereoelectroecephalography without a computed tomography scan for referencing: analysis of accuracy. Int J Med Robot e1888. https://doi.org/10.1002/rcs.1888
37. Talairach J, Bancaud J, Bonis A, Szikla G, Tournoux P (1962) Functional stereotaxic exploration of epilepsy. Confin Neurol 22: 328–331.
38. Taussig D, Chipaux M, Lebas A, Fohlen M, Bulteau C, Ternier J, Ferrand-Sorbets S, Delalande O, Dorfmüller G (2014) Stereoelectroencephalography (SEEG) in 65 children: an effective and safe diagnostic method for pre-surgical diagnosis, independent of age. Epileptic Disord 16:280–295.
39. Taussig D, Dorfmuler G, Fohlen M, Jalin C, Bulteau C, FerrandSorbets S, Chipaux M, Delalande O (2012) Invasive explorations in children younger than 3 years. Seizure 21:631–638.
40. Van der Loo E, Scijns OEMG, Hoogland G, Colon AJ, Wagner GL, Dings JTA, Kubben PL (2017) Methodology, outcome, safety and in vivo accuracy in traditional frame-based stereoelectroencephalography. Acta Neurochir 159:1733–1746.
41. Verburg N, Baayen JC, Idema S, Klitsie MA, Claus S, de Jonge CS, Vandertop P, de Witt Hamer PC (2016) In vivo accuracy of a frameless stereotactic drilling technique for diagnostic biopsies and stereoelectroencephalography depth electrodes. World Neurosurg 87:392–398.

Comments

The authors describe their initial clinical experience after performing robot-assisted-stereo-EEG in pediatric cohort of 14 patients. Prospective data concerning complications, usefulness, and accuracy have been collected and evaluated. Additionally, the authors discuss the problems and obstacles they have encountered during the establishment of an robotic arm. They also propose different solutions, which may help other centers overcome the initial difficulties with this technique. This is an obviously honest paper concerning a demanding group of pediatric epilepsy patients, who need invasive presurgical monitoring. As the authors state by themselves, ""they intend to describe the surgical technique"" and the provided technical information can be very valuable for other centers starting to use a robotic arm. I am concerned about the number of CT scans associated with this procedure, especially in a pediatric population. At least three scans are needed (preoperative CT angio, during the procedure, and postoperatively) and in some cases with fiducial displacement even more scans may be required. The authors commented on these issues, but to my mind it remains an issue. Thus, further development should also aim for further reduction of radiation in such procedures.

Hans Clusmann
Aachen, Germany

Source: Candela-Cantó, S., Aparicio, J., López, J.M. *et al*. Acta Neurochir (2018) 160: 2489. https://doi.org/10.1007/s00701-018-3720-8.

"Dirty Coagulation" Technique as an Alternative to Microclips for Control of Bleeding from Deep Feeders During Brain Arteriovenous Malformation Surgery

Danil A. Kozyrev[1,2], Peeraphong Thiarawat[1], Behnam Rezai Jahromi[1], Patcharin Intarakhao[1], Joham Choque-Velasquez[1], Ferzat Hijazy[1], Mario K. Teo[1,3], Juha Hernesniemi

Abstract

Meticulous haemostasis is one of the most important factors during microneurosurgical resection of brain arteriovenous malformation (AVM). Controlling major arterial feeders and draining veins with clips and bipolar coagulation are well-established techniques, while managing with bleeding from deep tiny vessels still proves to be challenging. This technical note describes a technique used by the senior author in AVM surgery for last 20 years in dealing with the issue highlighted. "Dirty coagulation" is a technique of bipolar coagulation of small feeders carried out together with a thin layer of brain tissue that surrounds these fragile vessels. The senior author uses this technique for achieving permanent haemostasis predominantly in large and/or deep-seated AVMs. To illustrate the efficacy of this technique, we retrospectively reviewed the outcome of Spetzler-Martin (SM) grade III-V AVMs resected by the senior author over the last 5 years (2010–2015). Thirty-five cases of AVM surgeries (14 SM grade III, 15 SM grade IV and 6 SM grade V) in this 5-year period were analysed. No postoperative intracranial haemorrhage was encountered as a result of bleeding from the deep feeders. Postoperative angiograms showed com-

Danil A. Kozyrev (✉)
e-mail: danilkozyrev@gmail.com
[1]Department of Neurosurgery, Helsinki University Hospital, Topeliuksenkatu 5, 00260 Helsinki, Finland
[2]Department of Paediatric Neurology and Neurosurgery, North-Western State Medical University, St. Petersburg, Russia
[3]Department of Neurosurgery, Bristol Institute of Clinical Neuroscience, North Bristol University Hospital, Bristol, UK

plete resection of all AVMs, except in two cases (SM grade V and grade III). "Dirty coagulation" provides an effective way to secure haemostasis from deep tiny feeders. This cost-effective method could be successfully used for achieving permanent haemostasis and thereby decreasing postoperative haemorrhage in AVM surgery.

Keywords Arteriovenous malformation, Bipolar coagulation, Microneurosurgery, Neurosurgical trick

Background

Resection of high-grade cerebral arteriovenous malformations (AVMs) is considered amongst the most complex and difficult in neurovascular surgeries. Some of the major problems are caused by not achieving permanent haemostasis in large and/or deep-seated lesions, commonly due to the small fragile feeders with a tendency to retract and hide inside white matter, and therefore resistant to simple coagulation. Furthermore, due to the very irregular elastic lamina, bipolar coagulation of these small fragile feeder vessels has proved ineffective, as they commonly stick to the bipolar forceps. One of the strategies described was the application of miniclips or microclips to manage these fragile vessels. However, if many microclips are used, orientation in the surgical field becomes more difficult and the risk of accidently tearing the vessels increases due to inadvertent manipulation of the clips. Different strategies have been developed, including the "dirty coagulation" technique, to deal with this problem when resecting brain AVM. Even though the technique might not seem elegant, it has proven to be effective.

This article describes the "dirty coagulation" technique in the microneurosurgical management of AVM and reviews the results of complex AVM resection by the senior author in the last 5 years to illustrate the efficacy based on intraoperative videos, radiological reports and clinical outcomes.

Methods

Clinical Material

From an extensive database of more than 1,200 AVMs treated in Helsinki and Kuopio, Finland, we retrospectively analysed AVM resections over a 5-year period (from September 2010 to June 2015) in view of the availability of high-definition quality videos. During this time, the senior author operated on 62 patients harbouring supratentorial and infratentorial AVMs. All the cases were categorised according to the Spetzler-Martin (SM) grading system [11]. We then selected 35 cases of SM grade III-V AVMs with intraoperative videos available for review. These high-grade cases were selected as they were most challenging in eliminating these tiny but extremely fragile feeder vessels. The data were collected under the approval of a local university hospital ethics committee (469/E0/04 HUCH).

Surgical Technique

During dissection of the AVM nidus, often in the deeper part, a neurosurgeon encounters the tiny fragile feeder vessels that are not amenable to the conventional method of coagulation. At this stage, we would apply the "dirty coagulation" technique. The basic idea of this technique is to use coagulum from the surrounding brain tissue with the vessel for stabilising bleeding. The "dirty coagulation" technique is executed through grabbing a small amount of tissue by bipolar tips and performing slow coagulation. This process takes some time, but if it is done too quickly the tiny feeders may shrink and retract back into the white matter. Thereby, the coagulum of tissue occludes the vessel lumen (Fig. 1). This helps to control bleeding and achieve permanent haemostasis.

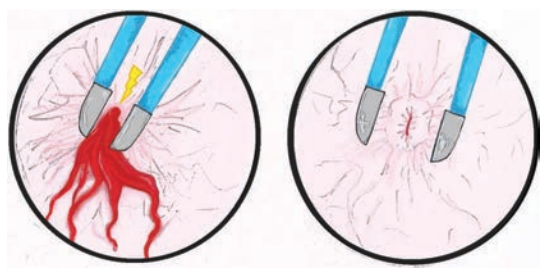

Fig. 1: Illustrations on the principle of the "dirty coagulation" technique to control deep arterial feeders using coagulum from the surrounding brain tissue with the vessel to achieve haemostasis.

To perform this, we prefer the Malis bipolar system (Codman, Raynham, MA, USA), usually using blunt forceps, with 2.0 mm tips and a bipolar setting of 25; and occasionally sharp forceps with a bipolar setting of 15–20. Generally, the blunt bipolar forceps are less susceptible to sticking of the fragile feeder vessels in comparison to the sharp forceps. In our practice, we use regular bipolar forceps. The special features to prevent stickiness include using extremely clean and cold forceps. To achieve this, cold saline can be used to clean the forceps. Additionally, several pairs of similar forceps are available on the operating table, to increase operative efficacy by ensuring at least a pair of clean forceps are available at all times. The "dirty coagulation" is also executed in a gentle manner under extreme concentration to eliminate damaging the surrounding tissue.

Some Features of Intraoperative and Postoperative Care

Generally, during AVM resections, we typically positioned the head 15–20 cm above the heart, ensuring no impairment of cerebral venous return. Mainly, semi-sitting or sitting positions are preferred, if feasible, according to localisation of the lesion. Systolic blood pressure (SBP) is maintained usually at the level of 100 mmHg. In some cases, when we encountered difficulties to coagulate the bleeding vessel, careful decrease of SBP to 60–70 mmHg for a short interval can help to achieve stable coagulation. This period can be prolonged up to 20–25 min if SBP is maintained around 80 mmHg. If during surgery we encountered a huge number of deep fragile vessels and dirty coagulation is heavily used, postoperatively such patients are maintained in a controlled moderate hypotensive state (100–120 mmHg) for several days. In selective cases, even deep arterial hypotension (80–100 mmHg) can be used in the postoperative period for the same reason.

Results

The "dirty coagulation" technique was utilised in all 35 patients with grade III-V grade AVMs (*see* Video, Supplemental Digital Content 1 and Fig. 2). Patient characteristics, radiological features and postoperative bleeding in the resection bed are presented in the Table 1. Two patients

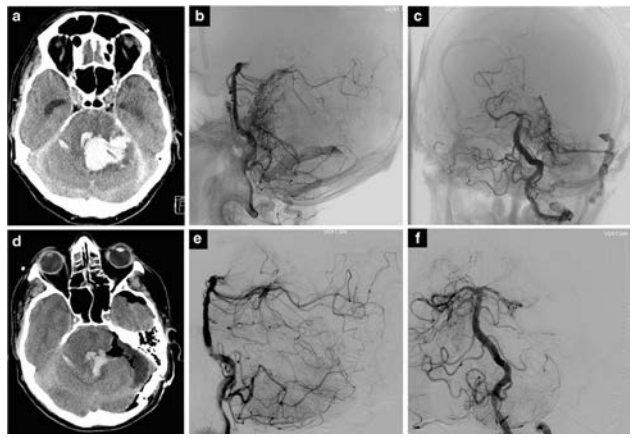

Fig. 2: *Illustrative case 1*. **a** Computed tomographic (CT) brain scan showed a large posterior fossa haematoma with hydrocephalus as evidenced by the enlarged temporal horns of the lateral ventricles, **b** and **c** Digital subtraction angiography (DSA), revealed a large left posterior fossa AVM with superior cerebellar artery and pontine arterial feeders, and early venous drainage to the left sigmoid sinus. **d** CT brain showed a well-decompressed posterior fossa, evacuation of the cerebellar haematoma with resolution of hydrocephalus. **e** and **f** DSA. Complete resection of the AVM was also achieved incorporating the "dirty coagulation" techniques to deal with small deep fragile feeders, and no AVM nidus or early venous drainage seen in the postoperative DSA.

Table 1: The characteristics and radiological features of 35 patients with AVMs of SM grade III-V with application of the "dirty coagulation" technique.

Mean age (range), years	40.2 (11–68)
Males:females, *n*	22:13
Grades of AVMs, *n*	
III	14
IV	15
V	6
Ruptured:unruptured, *n*	14:21
Final-check angiogram (DSA, MRI, CT), *n*	
Complete occlusion	33
Residual	2[a]
Postoperative haemorrhage in resection bed, *n*	0[b]

[a]One patient underwent multistage treatment (published elsewhere); another patient, with posterior midbrain AVM, had a small residual and underwent radiosurgery
[b]One patient had postoperative bleed due to ruptured of an unrecognised pericallosal aneurysm; another patient showed bilateral thin subdural haematomas after resection of a giant AVM

had residual AVMs after the first operation. One patient with giant central SM grade-V AVM underwent four microneurosurgical operations and four embolisations [6]. Another patient with posterior midbrain SM grade-III AVM showed a small remnant in the postoperative period. This patient subsequently underwent radiosurgical treatment of the AVM remnant. No postoperative intracranial haemorrhage was encountered as a result of bleeding from the deep feeders. One patient with angiographically proven complete resection of SM grade-IV callosal AVM had postoperative subarachnoid haemorrhage due to rupture of a proximal pericallosal aneurysm. Another patient, after removal of an SM grade-V giant frontal AVM, had thin bilateral subdural haematomas. This patient did not need reoperation and was treated conservatively. No operative mortality related to the described technique was encountered.

Discussion

In selective cases, microsurgical resection of the AVM remains the "gold standard" treatment modality that offers immediate AVM obliteration and a high curative rate [8, 10, 13]. We believe that surgical management of AVM remains one of the most challenging operations for the neurosurgeons, particularly when intraoperative AVM ruptures [16]. Torne *et al.* [14] classified causes of intraoperative AVM rupture in three categories: torn feeders, nidal penetration and premature venous occlusion.

From the senior author's experience, the torn feeders are the most difficult bleeding cause to control, particularly from the small fragile feeder vessels [3], and tamponade with small cotton balls is usually inadequate to control the bleeding. In many cases, these feeders arise from the deep part of the brain parenchyma and in close proximity to the ventricular systems [2]. Application of the "dirty coagulation" technique for small paraventricular vessels is difficult and usually ineffective as the ependymal layer fails to stabilise coagulation.

Morgan [7] proposed an elegant strategy of early access to the deep component of AVM to occlude the deep arterial feeders. When practical, this reduces the inflow to the nidus, and therefore circumferential spiral dissection of the AVM becomes less challenging as the nidus is softened. Alternatively, the large deep arterial feeders can also be occluded by endovascular methods to achieve the same purpose, and reduce the haemorrhagic risk of AVM surgery when resecting high-grade lesions. However, these techniques do not address the haemorrhagic risk from small tiny arterial feeder vessels. As a result, the management of tiny fragile feeding vessels at depth remained problematic.

Perinidal capillaries and tiny arterial feeders that surround the nidal have irregular elastic lamina [9]. Therefore, managing such vessels with direct bipolar coagulation is usually ineffective in stopping bleeding. Some authors proposed to control bleeding from these tiny fragile feeder vessels using miniclips and microclips [1, 12]. However, employment of this technique is difficult. For example, in large AVM surgery, application of many microclips might impair the visualisation of the nidal margin and render further resection problematic. Potentially the clips can be displaced during manipulation and caused shearing of the fragile feeder vessels. In addition, the use of microclips might pose the long-term risk of clip migration as previously reported [1].

Additional to microclips, tiny balls of oxidised cellulose covered by cottonoids could be used to tamponade the bleeding point, and occasionally the cotton balls held in place using self-retraining brain retractors. Combination of various strategies might be required in selective cases. Sometimes lower-grade AVMs also have these tiny vessels. In our opinion, the "dirty coagulation" technique described here using bipolar coagulation is sufficient and effective in dealing with such problems of controlling bleeding from these tiny fragile feeders. These small feeders, if not handled appropriately, can lead to the most devastating complication of AVM surgery: postoperative haematoma that could cause high morbidity and mortality. The application of the "dirty coagulation" technique can also be employed for removal of highly vascularised tumours (for example, malignant gliomas). Despite the fact that we did not encounter haemorrhagic complications related to the application of "dirty coagulation" technique, our series is relatively small and does not allow us to make an unambiguous statement about the effectiveness of the method. Perioperative bleeding complications after surgical treatment vary from 0 to 12.8% in different series [4, 5, 15]. As we analysed only cases with available high-definition quality videos, our series included only 35 cases that were performed during the last 5 years. Thereby, due to the relatively small number of cases in our series, we could not make a conclusion of a general nature about the bleeding risks. For comprehensive analysis, further investigation is needed.

This article describes the "dirty coagulation" technique in the microneurosurgical management of AVM and review of results of complex AVM resection by the senior author in the last 5 years proved its efficacy as no postoperative haematoma was encountered as a result of bleeding from the deep feeders.

Conclusions

The "dirty coagulation" technique has proved to be reliable, effective and safe in dealing with the tiny fragile deep feeders, and thereby to achieve permanent haemostasis in complex AVM surgery.

Acknowledgments We would like to thank Yaroslava A. Kozyreva for the drawings in this article.

Compliance with ethical standards

Funding No funding was received for this research.

Conflict of interest Professor Juha Hernesniemi is an Aesculap counsellor. All other authors certify that they have no affiliations with or involvement in any organisation or entity with any financial interest (such as honoraria; educational grants; participation in speakers' bureaus; membership, employment, consultancies, stock ownership, or other equity interest; and expert testimony or patent-licensing arrangements), or non-financial interest (such as personal or professional relationships, affiliations, knowledge or beliefs) in the subject matter or materials discussed in this manuscript.

For this type of study formal consent is not required.

Informed consent Informed consent was obtained from all individual participants included in the study.

This article does not contain any studies with human participants performed by any of the authors.

References

1. Chen CC, Zinn PO, Kasper EM, Ogilvy CS (2010) Cranio-spinal migration of a metallic clip placed during arteriovenous malformation resection—a case report, review of the literature, and management strategies. BMC Neurol 10:109.
2. Du R, Keyoung HM, Dowd CF, Young WL, Lawton MT (2007) The effects of diffuseness and deep perforating artery supply on outcomes after microsurgical resection of brain arteriovenous malformations. Neurosurgery 60:638–646, discussion 646–638.

3. Hernesniemi J, Romani R, Lehecka M, Isarakul P, Dashti R, Celik O, Navratil O, Niemela M, Laakso A (2010) Present state of microneurosurgery of cerebral arteriovenous malformations. Acta Neurochir Suppl 107:71–76.
4. Javadpour M, Al-Mahfoudh R, Mitchell PS, Kirollos R (2016) Outcome of microsurgical excision of unruptured brain arteriovenous malformations in ARUBA-eligible patients. Br J Neurosurg 30:619–622.
5. Korja M, Bervini D, Assaad N, Morgan MK (2014) Role of surgery in the management of brain arteriovenous malformations: prospective cohort study. Stroke 45:3549–3555.
6. Kozyrev DA, Jahromi BR, Hernesniemi J (2016) Total temporary occlusion of blood flow for several hours to treat a giant deep arteriovenous malformation: a series of multiple operations to save a young life. Surg Neurol Int 7:79.
7. Morgan MK (2014) Surgical strategies for Brain AVM. In: Misra BK, Laws ER, Kaye AH (eds) Current progress in neurosurgery. Three Life Media, Mumbai, pp 212–213.
8. Potts MB, Lau D, Abla AA, Kim H, Young WL, Lawton MT, Project UBAS (2015) Current surgical results with low-grade brain arteriovenous malformations. J Neurosurg 122:912–920.
9. Sato S, Kodama N, Sasaki T, Matsumoto M, Ishikawa T (2004) Perinidal dilated capillary networks in cerebral arteriovenous malformations. Neurosurgery 54:163–168, discussion 168–170.
10. Schramm J, Schaller K, Esche J, Bostrom A (2016) Microsurgery for cerebral arteriovenous malformations: subgroup outcomes in a consecutive series of 288 cases. J Neurosurg. doi:10.3171/2016.4. JNS153017.
11. Spetzler RF, Martin NA (1986) A proposed grading system for arteriovenous malformations. J Neurosurg 65:476–483.
12. Sundt TM Jr, Kees G Jr (1986) Miniclips and microclips for surgical hemostasis. Technical note. J Neurosurg 64:824–825.
13. Teo MK, Young AM, St George EJ (2016) Comparative surgical outcome associated with the management of brain arteriovenous malformation in a regional neurosurgical centre. Br J Neurosurg 1–8.
14. Torne R, Rodriguez-Hernandez A, Lawton MT (2014) Intraoperative arteriovenous malformation rupture: causes, management techniques, outcomes, and the effect of neurosurgeon experience. Neurosurg Focus 37:E12.
15. Wong J, Slomovic A, Ibrahim G, Radovanovic I, Tymianski M (2017) Microsurgery for ARUBA Trial (a randomized trial of unruptured brain arteriovenous malformation)—eligible unruptured brain arteriovenous malformations. Stroke 48:136-144.
16. Yaşargil MG (1988) Microneurosurgery, vol IIIB. Thieme, New York.

Comments

This is a technique that Dr. Hernesniemi is known to have pioneered and promoted. When introduced it defied the conventional wisdom, at the time, of fine bipolar technique applied to the vessel with no collateral damage to be inflicted on surrounding tissue. However, for AVM this technique often fails for reasons presented in this paper and this "dirty coagulation" technique is necessary. It is important for those charged with the care of AVM to be aware of this technique and who first promoted its use. I have seen Dr. Hernesniemi use this and have adopted this technique, where appropriate, for my own AVM cases.

Michael Kerin
Morgan, Australia

I think this is a helpful contribution because it shows the way to a very useful, albeit counterintuitive technique for coagulating tiny vessels. I have used this technique for decades and never bothered to write about it because it is so obviously the only technique that works in the deep white matter around AVMs. I am sure that this technique has been used by many other AVM surgeons also because it is a logical development. As it has been demonstrated, the intuitive decision to use fine-tipped forceps for fine vessels is wrong for fine vessels in the white matter around AVM, just as many other spontaneous intuitive decisions made by medical doctors.

Microclips are a good alternative method, but I can confirm many of the observations the authors have made: too many microclips soon turn out to be in the way when dealing with other small feeders. These difficult feeders in deep become more common the closer one is to the ependyma of the ventricle. The microclips produce short-cuts when bipolar is used close to them and they can shear off. This reviewer also confirms that the use of broader bipolar tips is very useful, because the current flow is not so focused as in finely tipped bipolar forceps. Thus, sticking to the coagulated vessel is less frequent when using broader tipped forceps. This somehow automatically leads to the technique that these authors have named "dirty coagulation". A major part of the trick of "dirty coagulation" is to include some tissue around the vessel between the two forceps tips (as described) but also to use a not too high current and take some time with a low flow of electric current in order to allow the tissue to shrink slowly and desiccate slowly. The speed of shrinking and desiccation is an important feature, because if this happens too quickly these fragile feeders may tear 2–3 mm away from the coagulation forceps because they are torn away.

The apparently logical step of using very fine forceps and only enclosing the tiny vessel just does not work in the deep white matter around AVM. This reviewer has used blunt forceps 95% of the time during his own large AVM series [10]. The counterintuitive step of using broad-tipped forceps turns out to be more effective and better suited.

Johannes Schramm
Bonn, Germany

Source: Kozyrev, D.A., Thiarawat, P., Jahromi, B.R. *et al*. Acta Neurochir (2017) 159: 855. https://doi.org/10.1007/s00701-017-3138-8.

Examination of the Upper Limb

Amgad S. Hanna

Motor Examination

Muscles are tested and graded using the MRC system: 0: no function, 1: flicker, 2: movement with gravity eliminated, 3: movement against gravity, 4: movement against some resistance, and 5: normal. Detailed testing can be done using a hydraulic hand dynamometer. Range of motion can be tested with a goniometer.

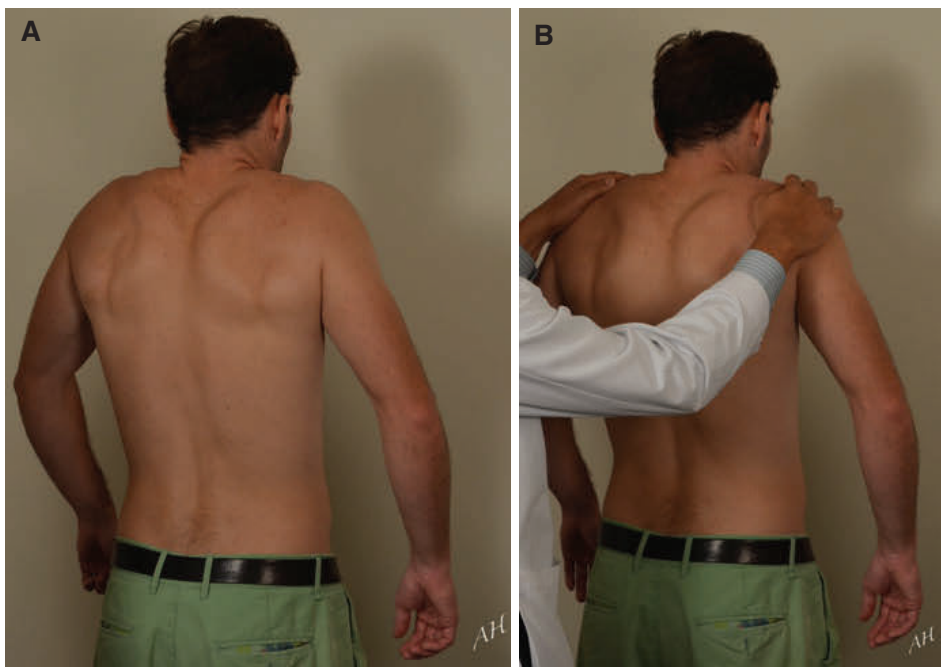

Fig. 1: Trapezius (spinal accessory n). Ask the patient to shrug the shoulders (**A**), then against resistance (**B**).

Electronic supplementary material: The online version of this chapter (doi: 10.1007/978-3-319- 39694-1_23) contains supplementary material, which is available to authorized users

Amgad S. Hanna
Department of Neurosurgery, University of Wisconsin, Madison, USA

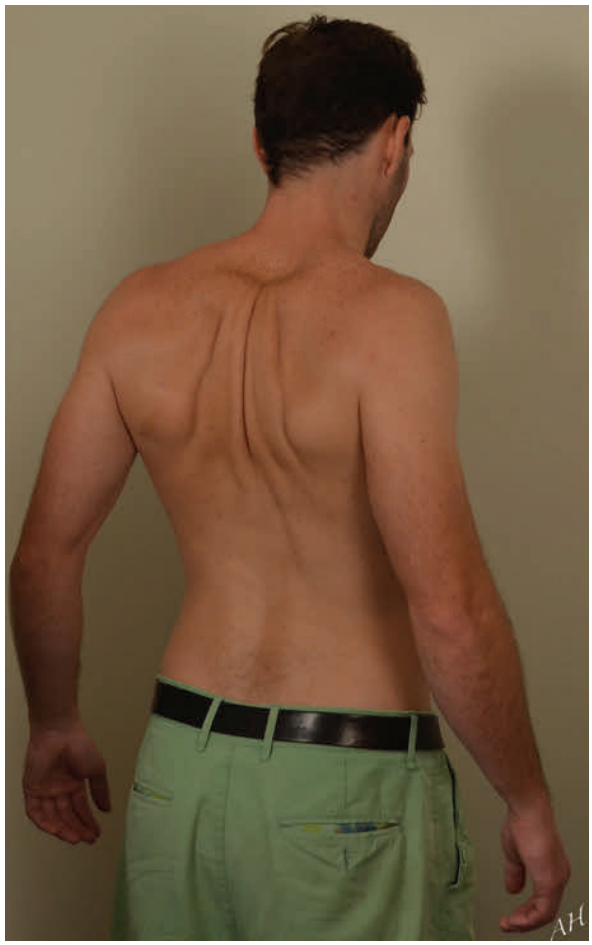

Fig. 2: Rhomboids (dorsal scapular n). Ask the patient to retract the shoulder blades towards the midline as in a military position.

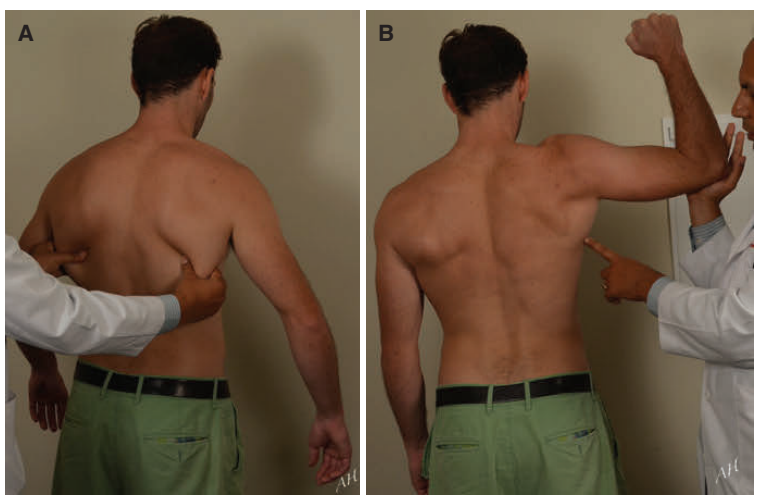

Fig. 3: Latissimus dorsi (thoracodorsal n). (**A**) Ask the patient to cough while palpating the posterior axillary fold to assess for muscle contraction. (**B**) Ask the patient to adduct the shoulder against resistance from a 90° position with the elbow flexed.

Fig. 4: Teres major (lower subscapular n). Ask the patient to adduct the shoulder against resistance from a 90° position with the elbow fully extended.

Fig. 5: Teres minor (axillary n). Shoulder external rotation is tested by asking the patient to push backwards with his hand against resistance while the shoulder and elbow are at 90°.

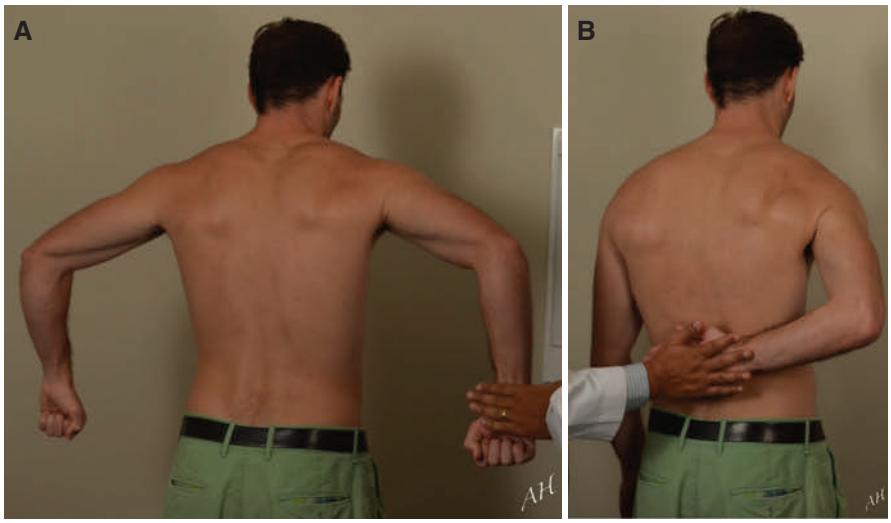

Fig. 6: Subscapularis (upper and lower subscapular nn). (**A**) Shoulder internal rotation is tested by asking the patient to push backwards with the hand against resistance while the shoulder and elbow are at 90°. (**B**) Gerber's lift-off test [1]: ask the patient to lift the hand off his back against resistance.

Fig. 7: Test for scapular winging. Ask the patient to push on the wall first with the elbows extended. (**A**) This tests for serratus anterior (long arms = long thoracic n). Ask the patient to take a step forward and push again with the elbows flexed. (**B**) This tests for the trapezius. (**A, B**) No scapular winging. (**C**) Right scapular winging due to long thoracic neuropathy.

Fig. 8: Shoulder abduction: (**A**) Initiation, especially in internal rotation (thumbs towards the floor), supraspinatus (suprascapular n). (**B**) Up to 90°, deltoid (middle fibers, axillary n). (**C**) Up to 180°, coupling of serratus anterior and trapezius. This movement is between the scapula and the chest wall.

Fig. 9: Posterior fibers of the deltoid (*arrow*). The patient is asked to push back while the shoulder is abducted at 90° and the elbow fully extended.

Fig. 10: Eyes need to be checked for the presence of Horner's syndrome. (**A**) Normal. (**B**) Right Horner's syndrome in a patient with right brachial plexus avulsion (preganglionic) injury. Note right ptosis and miosis.

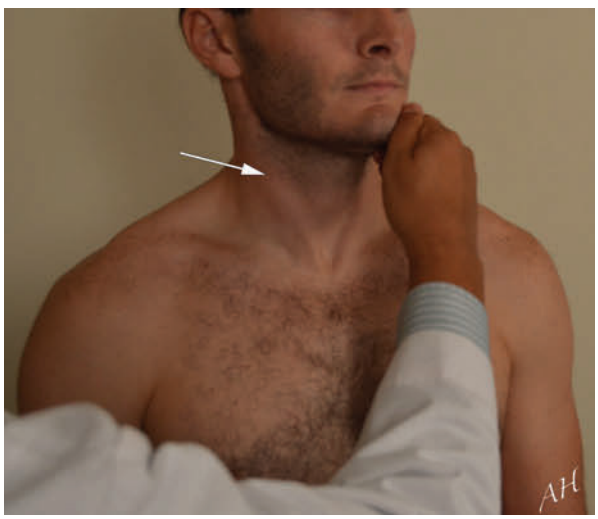

Fig. 11: Sternocleidomastoid (spinal accessory n). The patient is asked to push with his chin to the contralateral side against the examiner's hand. The sternocleidomastoid (*arrow*) is observed contracting.

Fig. 12: Anterior fibers of the deltoid.

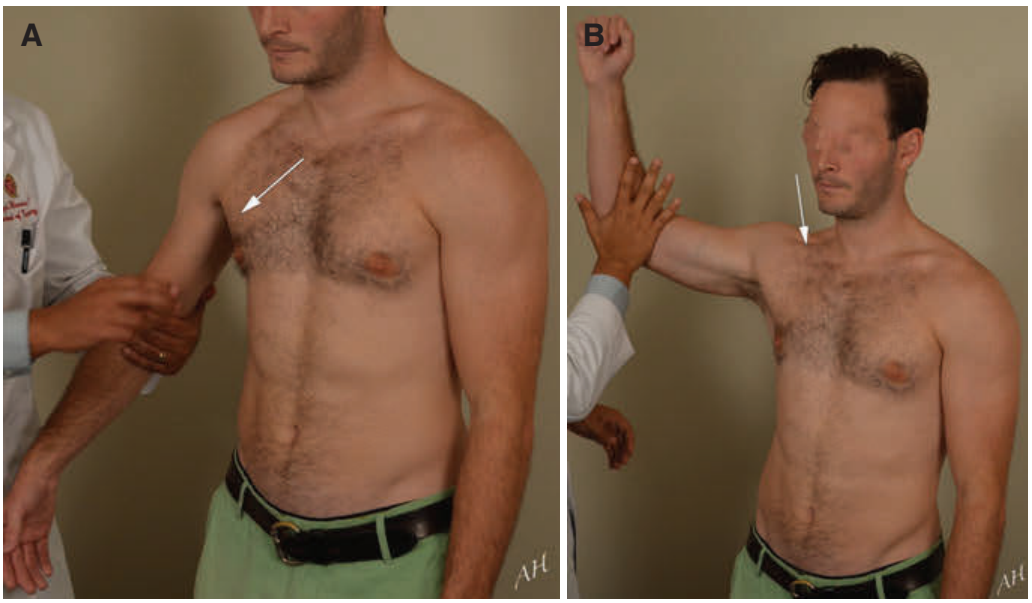

Fig. 13: Pectoralis major. (**A**) Sternal head. The patient is asked to adduct the shoulder against resistance; the sternal head of pectoralis major (*arrow*) is felt contracting along the anterior axillary fold. (**B**) Clavicular head. The patient is asked to protract (push forwards) the shoulder against resistance while the shoulder and elbow are at 90°. The clavicular head of pectoralis major (*arrow*) can be seen and felt contracting.

Fig. 14: Infraspinatus (suprascapular n). Shoulder external rotation is tested by asking the patient to push outwards against the examiner's hand while the elbow is flexed 90°.

Fig. 15: Subscapularis. Shoulder internal rotation is tested by asking the patient to push inwards against the examiner's hand while the elbow is flexed 90°.

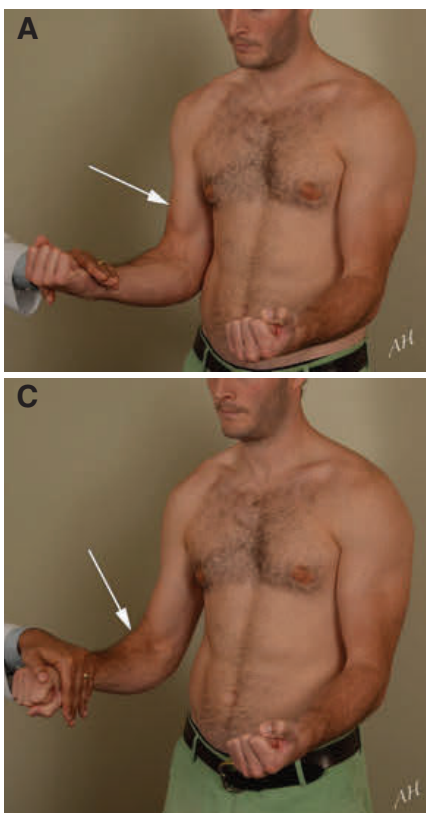

Fig. 16: Elbow flexion [1]. (**A**) With the forearm supinated: Biceps brachii (*arrow*) and brachialis (Musculocutaneous n). (**B**) In semi-prone position: brachioradialis (*arrow*) (radial n). (**C**) With the forearm pronated: Brachialis and brachioradialis (*arrow*).

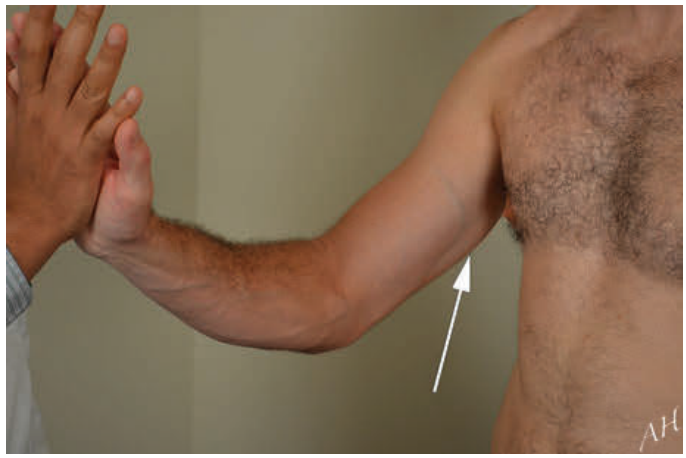

Fig. 17: Triceps (*arrow*) (radial n). The patient is asked to extend the elbow against resistance.

Fig. 18: Supinator (radial n). The patient is asked to supinate against resistance, while the elbow is extended to minimize contribution from the biceps.

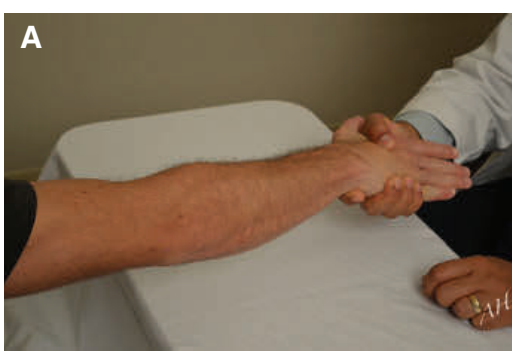

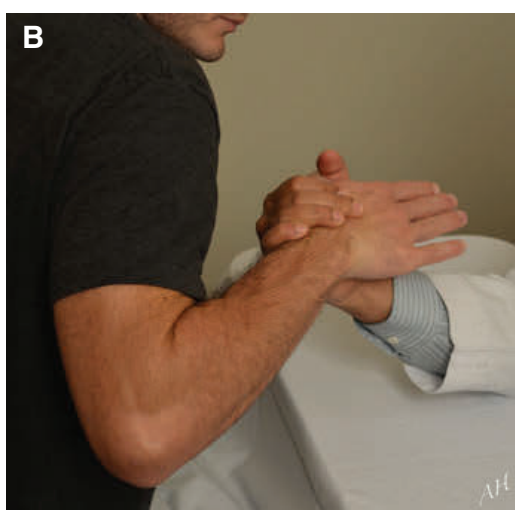

Fig. 19: Pronation. (**A**) Pronator teres (median n). The patient is pronating against resistance with the elbow extended. (**B**) Pronator quadratus (AIN). The patient is pronating against resistance with the elbow fully flexed.

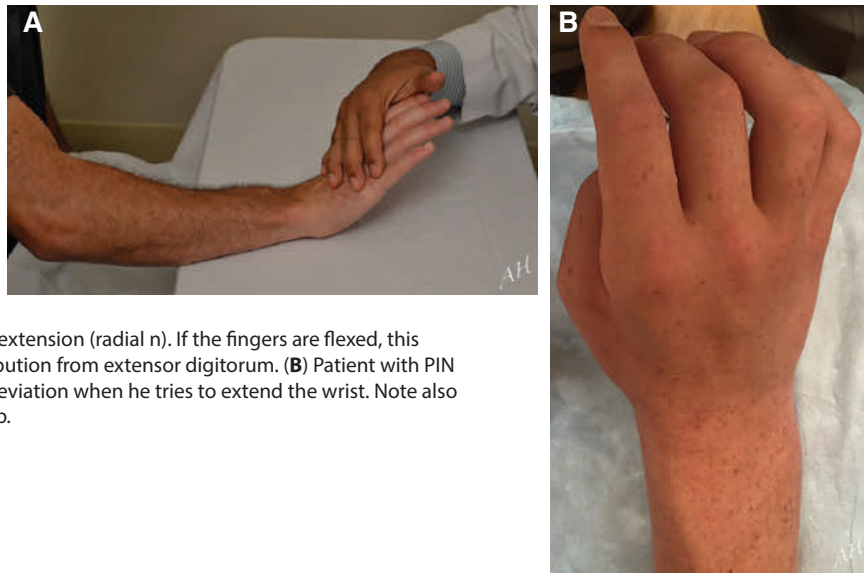

Fig. 20: (**A**) Wrist extension (radial n). If the fingers are flexed, this minimizes contribution from extensor digitorum. (**B**) Patient with PIN palsy has radial deviation when he tries to extend the wrist. Note also partial finger drop.

Fig. 21: Extensor digitorum (radial n). Finger extension (except thumb) is tested at the MPJ against resistance.

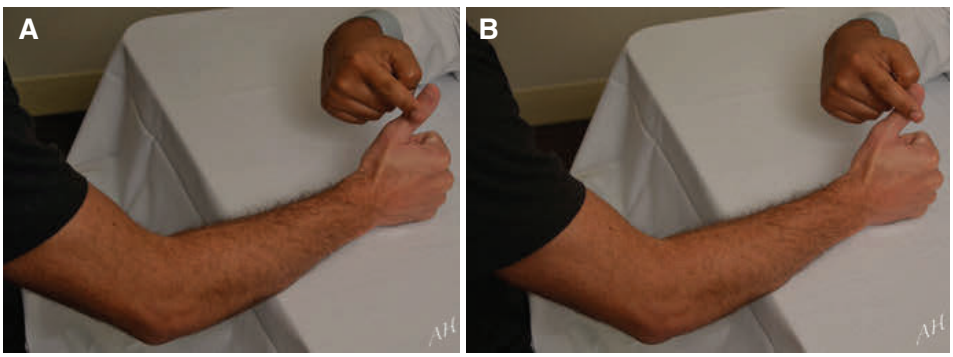

Fig. 22: Thumb extension (radial n). Ask the patient to extend the thumb [hitchhike], while (**A**) applying resistance at the proximal phalanx of the thumb: EPB, then (**B**) at the distal phalanx: EPL.

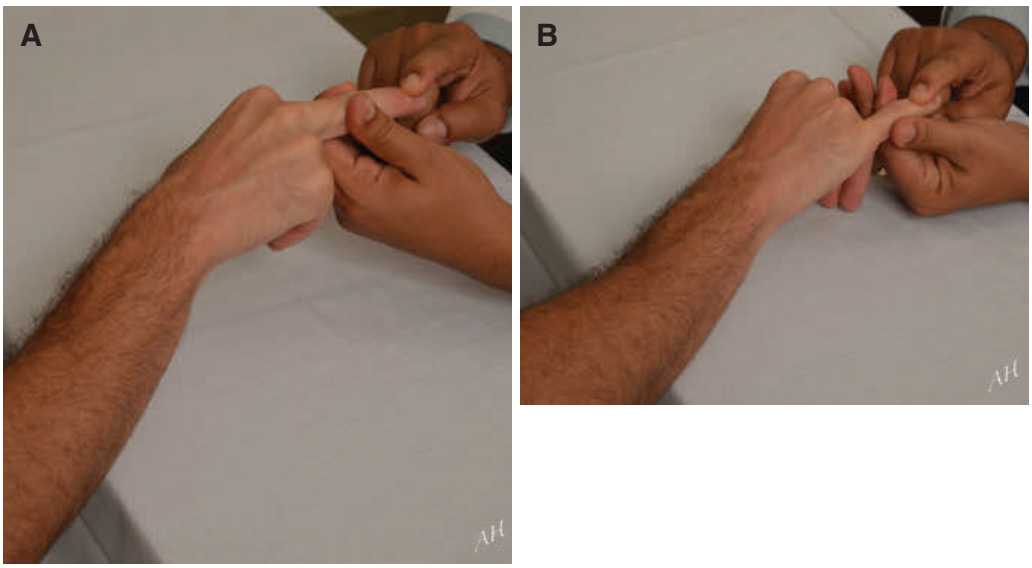

Fig. 23: Lumbricals: index and middle fingers ((**A**), median n), ring and little fingers ((**B**), ulnar n). Test finger extension at the IPJ against resistance.

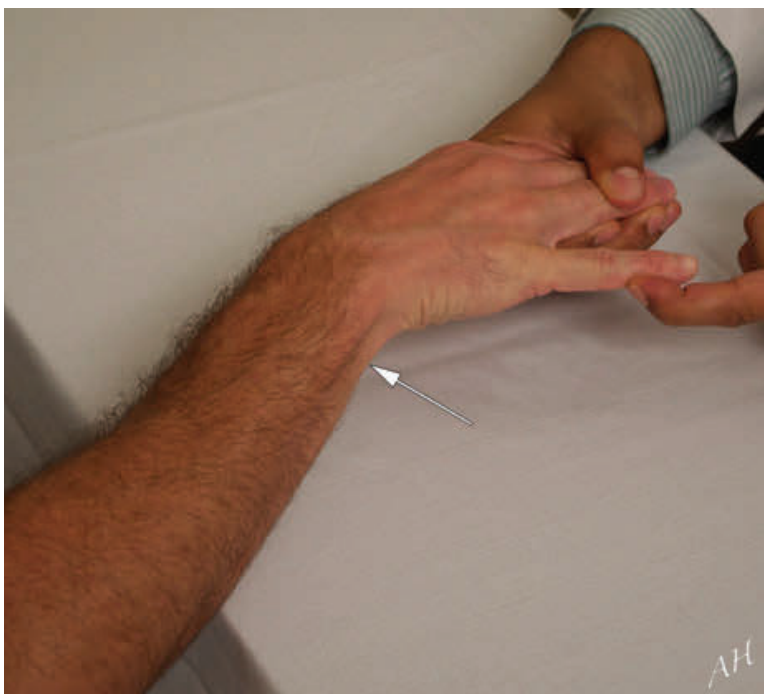

Fig. 24: Abductor digiti quinti (minimi) (ulnar n). Tested by abduction of the little finger against resistance. Also note contraction of the FCU (*arrow*, ulnar n) to stabilize the pisiform bone.

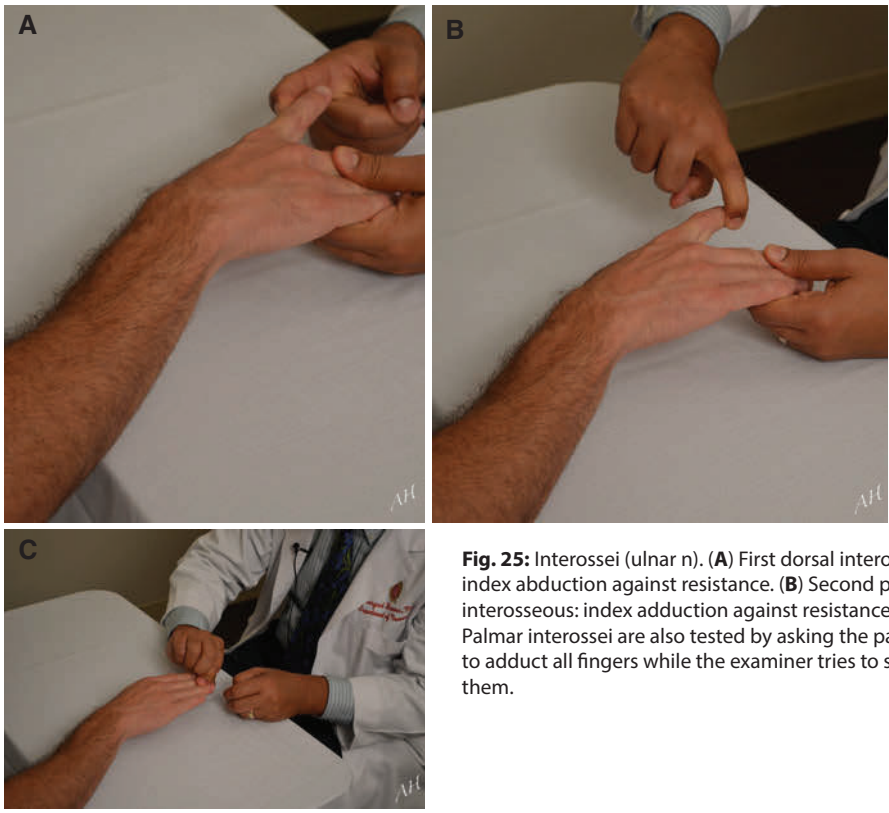

Fig. 25: Interossei (ulnar n). (**A**) First dorsal interosseous: index abduction against resistance. (**B**) Second palmar interosseous: index adduction against resistance. (**C**) Palmar interossei are also tested by asking the patient to adduct all fingers while the examiner tries to separate them.

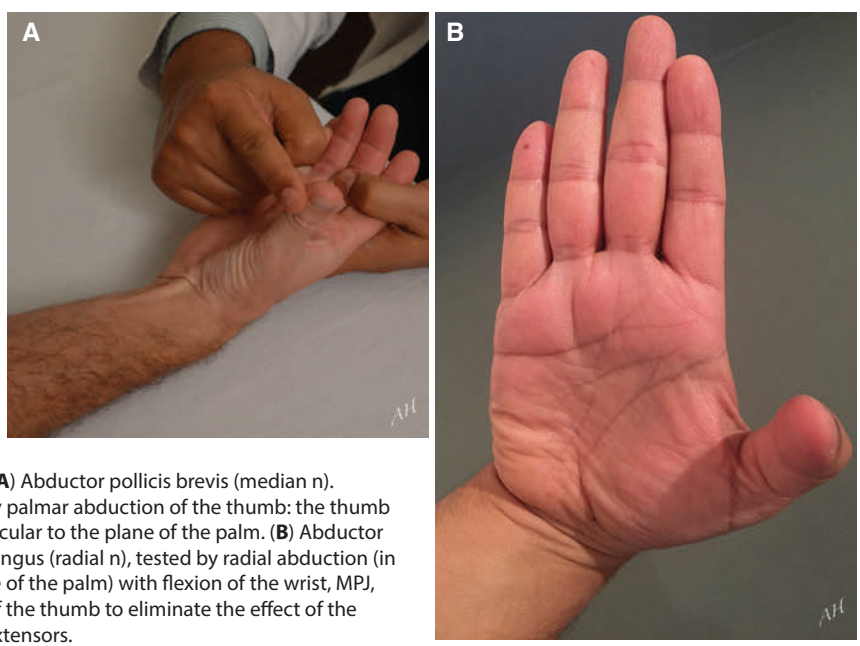

Fig. 26: (**A**) Abductor pollicis brevis (median n). Tested by palmar abduction of the thumb: the thumb perpendicular to the plane of the palm. (**B**) Abductor pollicis longus (radial n), tested by radial abduction (in the plane of the palm) with flexion of the wrist, MPJ, and IPJ of the thumb to eliminate the effect of the thumb extensors.

Fig. 27: Opponens pollicis (median n). The patient touches the thumb to the little finger while the examiner tries to separate them.

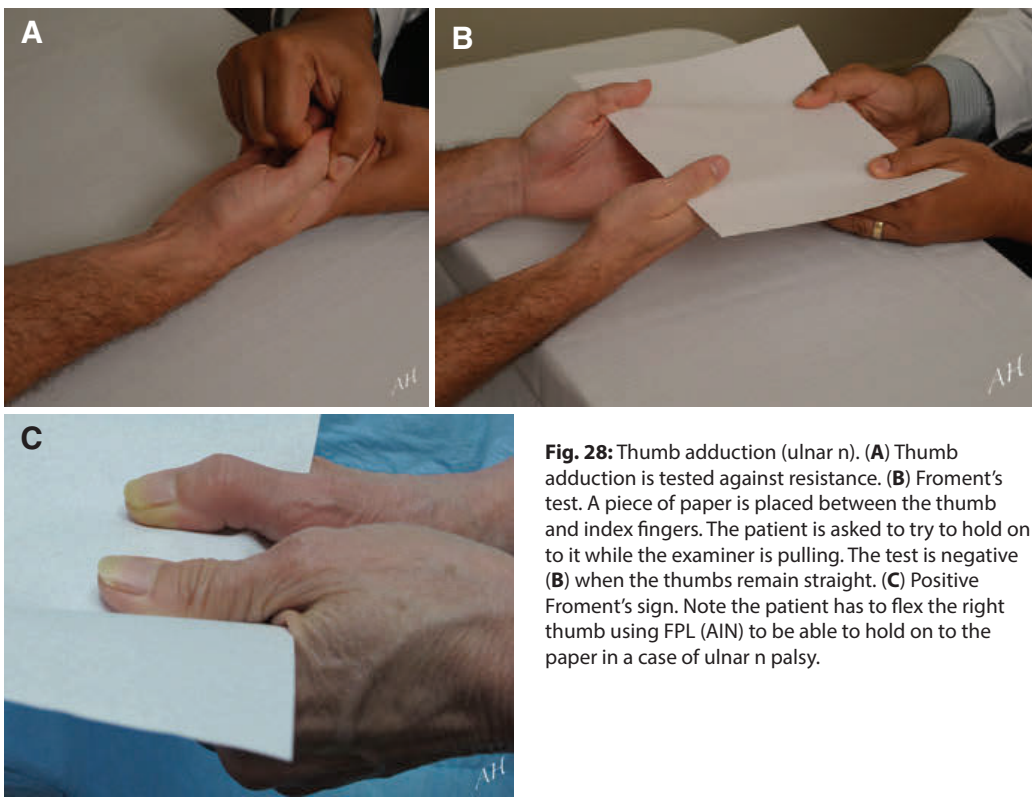

Fig. 28: Thumb adduction (ulnar n). (**A**) Thumb adduction is tested against resistance. (**B**) Froment's test. A piece of paper is placed between the thumb and index fingers. The patient is asked to try to hold on to it while the examiner is pulling. The test is negative (**B**) when the thumbs remain straight. (**C**) Positive Froment's sign. Note the patient has to flex the right thumb using FPL (AIN) to be able to hold on to the paper in a case of ulnar n palsy.

Fig. 29: (**A**) Flexor pollicis longus (AIN) flexion of the IPJ of the thumb against resistance. (**B**) The AIN is also tested by the ability to make the 'ok' sign. (**C**) In AIN palsy, the patient loses the ability to flex the IPJ of the thumb and the DIP of the index finger.

Fig. 30: Flexor digitorum profundus: index and middle fingers. ((**A**), AIN), ring and little fingers. ((**B**), ulnar n). Test flexion of the DIP against resistance.

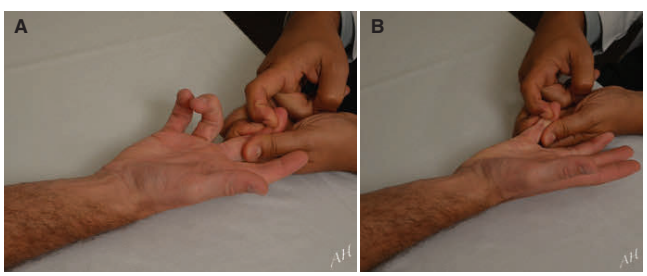

Fig. 31: Flexor digitorum superficialis (sublimis) (median n). The medial 4 fingers are tested for flexion at the PIP against resistance. To minimize the contribution from FDP, the remaining 3 fingers should be hyperextended by the examiner.

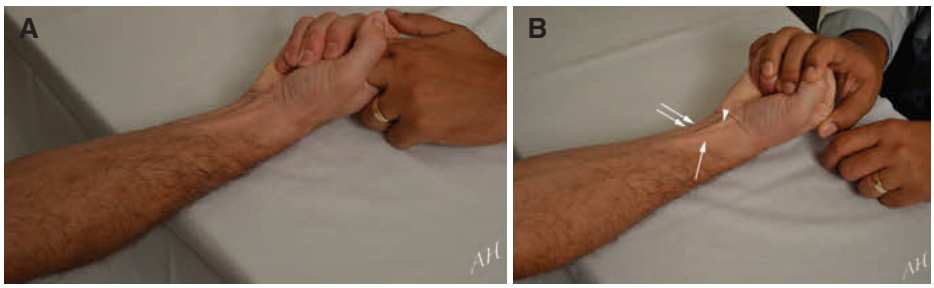

Fig. 32: Long flexor tendons (median and ulnar). (**A**) Ask the patient to squeeze your fingers. (**B**) Ask the patient to make a fist and flex the wrist. The contracting muscle tendons can be seen: flexor carpi radialis (*single arrow*), palmaris longus (*arrowhead*), and flexor carpi ulnaris (*double arrows*).

Fig. 33: Quantitative testing of hand motor strength. (**A**) Hydraulic hand dynamometer. (**B**) Grip testing. (**C**) Key pinch. (**D**) Palmar pinch. (**E**) Tip pinch.

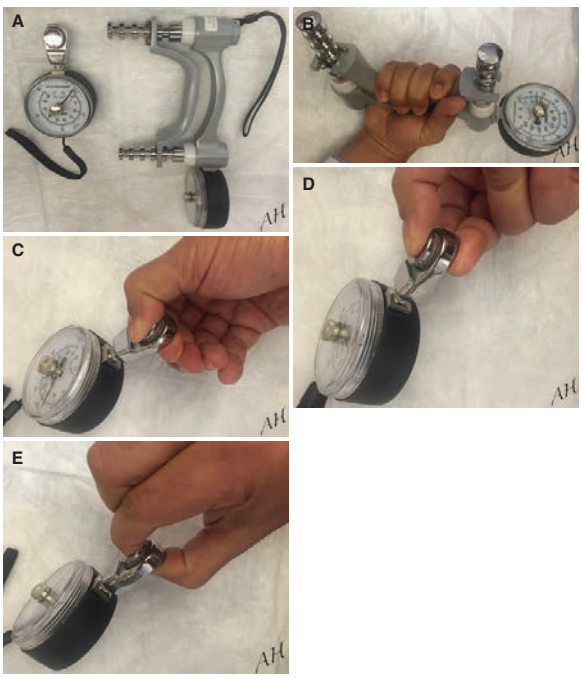

Fig. 34: A goniometer can be used to measure the range of motion more accurately.

Reflexes

Fig. 35: Brachioradialis reflex (C6) elbow at 120°. Tap towards the insertion of the brachioradialis tendon, preferably on your finger to avoid pain from tapping on the superficial radial n.

Fig. 36: Biceps reflex (C5, C6) elbow at 120°. Palpate the biceps tendon and tap on your finger.

Fig. 37: Triceps reflex (C6, C7) elbow at 90°, tap directly on the triceps tendon.

Sensory Examination

Sensation is routinely tested to light touch and pinprick. Detailed testing can include 2-point discrimination. Monofilaments of variable weight can be used especially in patients with peripheral neuropathy, e.g., diabetics [2].

Fig. 38: Upper lateral brachial cutaneous n (axillary n).

Fig. 39: Lower lateral brachial cutaneous n (radial n).

Fig. 40: Medial brachial cutaneous n (medial cord).

Fig. 41: Lateral antebrachial cutaneous n (musculocutaneous n).

Fig. 42: Medial antebrachial cutaneous n (medial cord).

Fig. 43: Palmar cutaneous branch (median n above the wrist). This branch is typically spared in carpal tunnel syndrome since it usually travels superficial to the transverse carpal ligament.

Fig. 44: Palmar digital nerves (median n). They supply the lateral 3.5 fingers (**A**–**D**) palmar surface and their middle and distal phalanges on the dorsal surface.

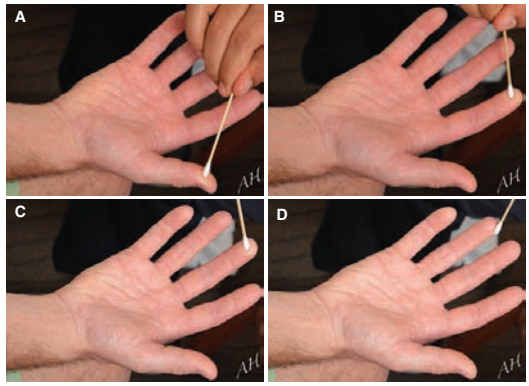

Fig. 45: Palmar cutaneous branch (ulnar n above the wrist).

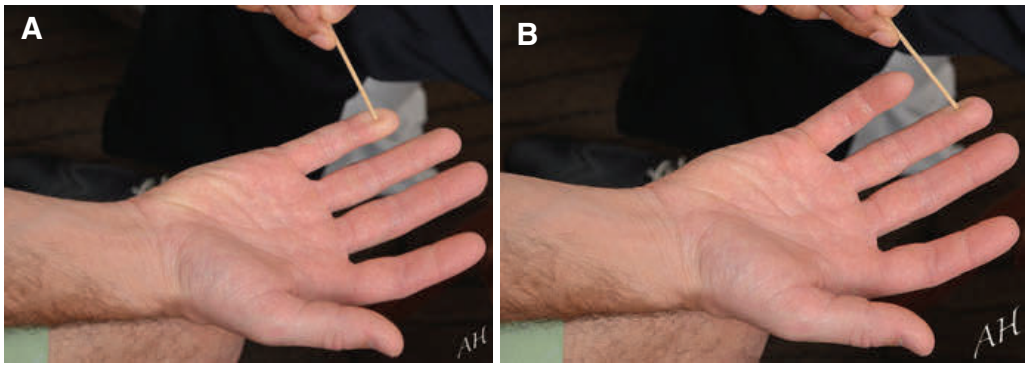

Fig. 46: Superficial terminal branch (ulnar n). It supplies the medial 1.5 fingers (**A, B**) palmar surface and the distal part of their dorsal surface.

Fig. 47: Dorsal cutaneous branch (ulnar n above the wrist). Typically spared if an ulnar n lesion is at the wrist (Guyon's canal).

Fig. 48: Superficial terminal branch (radial n).

Fig. 49: Posterior cutaneous n of the forearm (radial n).

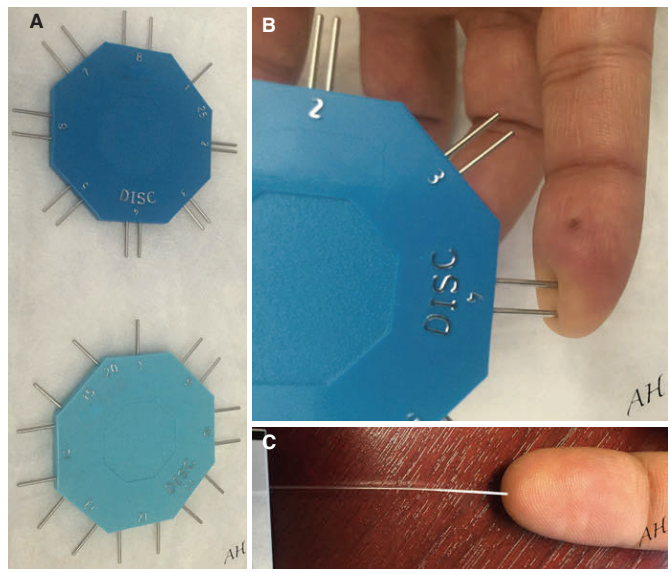

Fig. 50: (**A, B**) Two-point discrimination testing: normally 2–4 mm in the fingers. (**C**) 10 g monofilament testing [3]; if preserved in the foot, this is considered protective from neuropathic ulcers [4].

References

1. Gerber C, Krushell RJ (1991) Isolated rupture of the tendon of the subscapularis muscle. Clinical features in 16 cases. J Bone Joint Surg Br 73(3):389–394.
2. Kleiber T, Kunz L, Disselhorst-Klug C (2015) Muscular coordination of biceps brachii and brachioradialis in elbow flexion with respect to hand position. Front Physiol 6:215.
3. Weinstein S (1993) Fifty years of somatosensory research: from the Semmes-Weinstein monofilaments to the Weinstein enhanced sensory test. J Hand Ther 6(1):11–22, discussion 50.
4. Young D, Schuerman S, Flynn K, Hartig K, Moss D, Altenburger B (2011) Reliability and responsiveness of an 18 site, 10-g monofilament examination for assessment of protective foot sensation. J Geriatr Phys Ther 34(2):95–98.
5. The guarantors of brain (eds). Aids to the examination of the peripheral nervous system, 4th edn. Edinburgh: WB Saunders; 2000. pp 1–36.
6. Russell SM (2006) Examination of peripheral nerve injuries: an anatomical approach. Thieme, New York, pp 1–107.
7. Kendall FP, McCreary EK, Provance PG, Rodgers MM, Romani WA (2005) Muscles: testing and function with posture and pain, 5th edn. Lippincott Williams & Wilkins, Philadelphia.

Source: Hanna A.S. (2017) Examination of the Upper Limb. In: Nerve Cases. Springer, Cham.

Abbott

GUARDING HER EVERY MOMENT

START WITH

LEVESAM

Levetiracetam 250/500/750/1000mg Tablets • Levetiracetam Syrup/Injection 100mg/ml

EMPOWER HER

Pictures shown and are not of actual patients are for representational purpose only.

Abridged Prescribing Information: LEVESAM 250 / 500 / 750 / 1000

COMPOSITION: Each film-coated tablet contains levetiracetam 250 mg / 500 mg / 750 mg /1000 mg. INDICATION: Adjunctive therapy in the treatment of partial onset seizures in adults with epilepsy. DOSAGE AND ADMINISTRATION: (Patients > 16 yrs of age) : Treatment should be initiated with a daily dose of 1000 mg/day, given as twice-daily dosing (500 mg BID), with or without food. Additional dosing increments may be given (1000 mg/day additional every 2 weeks) to a maximum recommended daily dose of 3000 mg, depending upon the clinical response and tolerability. Elderly: Adjust dose in patients with compromised renal function. Renal impairment: Adjust dose according to creatinine clearance. Hepatic impairment: No dose adjustment with mild to moderate hepatic impairment. CONTRAINDICATION: Hypersensitivity to levetiracetam or any ingredient of the formulation. WARNINGS AND PRECAUTIONS: Keep out of reach of children. Central nervous system adverse events, viz. somnolence and fatigue, coordination difficulties, psychotic symptoms and behavioral abnormalities reported to occur most frequently within the first 4 weeks of treatment. Minor hematologic abnormalities also reported. May cause dizziness and somnolence and hence jobs which require extreme alertness should be avoided. Withdrawal of drug: Gradual withdrawal advised. Pregnancy: Should be used only if the potential benefit justifies the potential risk to the fetus. Nursing Mothers: Because of the potential for serious adverse reactions in nursing infants, physician's discretion advised. Drug Interactions: No clinically significant interactions reported. ADVERSE REACTIONS: The most frequently reported adverse reactions are asthenia, headache, infection, pain, anorexia, amnesia, anxiety, ataxia, depression, dizziness, emotional lability, hostility, nervousness, paresthesia, somnolence, vertigo, increased cough, pharyngitis, rhinitis, sinusitis, diplopia. HOW SUPPLIED / STORAGE: Blister pack of 10 tabs. Store in a cool, dry place, protected from light. Please read the full prescribing information before usage. Additional information available on request with the Medical Services Division, Abbott Healthcare Private Limited, 1st Floor, D Mart Building, Goregaon-Mulund Link Road, Mumbai 400080. Version: 1.06, Dt. 05-04-16

Abridged Prescribing Information: LEVESAM ORAL SOLUTION

COMPOSITION: Each 1 ml contains levetiracetam 100 mg. INDICATION: Adjunctive therapy in the treatment of partial onset seizures in adults in adults and children 4 years of age and older with epilepsy. DOSAGE AND ADMINISTRATION: (Patients > 4 years of age): Treatment should be initiated with a daily dose of 20 mg/day in 2 divided doses(10 mg/kg BID). The daily dose should be increased every 2 weeks by increments of 20 mg/kg to the recommended daily dose of 60 mg/kg, the daily dose may be reduced. Patients with body weight ≤20 kg should be dosed with oral solution. Levetiracetam is given orally with or without food. (Patients >16 yrs of age): Treatment should be initiated with a daily dose of 1000 mg/day, given as twice-daily dosing (500 mg BID), with or without food. Additional dosing increments may be given (1000 mg/day additional every 2 weeks) to a maximum recommended daily dose of 3000 mg. CONTRAINDICATION: Hypersensitivity to levetiracetam or any ingredient of the formulation. WARNINGS AND PRECAUTIONS: Keep out of reach of children. Central nervous system adverse events, viz. somnolence and fatigue, coordination difficulties, psychotic symptoms and behavioral abnormalities reported to occur most frequently within the first 4 weeks of treatment. Minor hematologic abnormalities also reported. May cause dizziness and somnolence and hence jobs which require extreme alertness should be avoided. Withdrawal of drug: Gradual withdrawal advised. Pregnancy: Should be used only if the potential benefit justifies the potential risk to the fetus. Nursing Mothers: Because of the potential for serious adverse reactions in nursing infants, physician's discretion advised. Drug Interactions: No clinically significant interactions reported. ADVERSE REACTIONS: The adverse events most frequently reported with the use of Levetiracetam in combination with other AEDs in pediatric patients were somnolence, accidental injury, hostility, nervousness and asthenia. The most frequently reported adverse events associated with the use of levetiracetam in combination with other AEDs in adults were somnolence, asthenia, infection and dizziness. Of the most frequently reported adverse events in adults were asthenia, somnolence and dizziness is reported to occur predominantly during the first 4 weeks of treatment with levetiracetam. HOW SUPPLIED / STORAGE: Syrup is available in bottle pack of 100 ml. Store in a cool, dry place, protected from light. Keep out of reach of children.

Please read the full prescribing information before usage. For additional information, please contact Medical Services Division, **Abbott Healthcare Pvt. Ltd.** Floor 18, Godrej BKC, Plot No. C–68, Near MCA Club, Bandra–Kurla Complex, Bandra East, Mumbai 400051. www.abbott.co.in Version : 1.0, Dt. 19.06.2014

INDLVM185007 28 NOV 2018